determining the statin resistance-responsible region of HCV and also for investigating the anti-HCV mechanism of statins in general.

In the present study, we demonstrated the diverse profiles of four HCV replicons to anti-HCV reagents. sKAH5R showed the lowest sensitivity to IFN-γ, IFN-λ, and statins (PTV, RSV, and FLV). In contrast, s1B-4R exhibited the highest level of sensitivity to IFN-λ and statins (PTV, RSV, and FLV). sKAH5R and s1B-4R possessed a sensitive and a resistant phenotype to various anti-HCV reagents. The nucleotide sequences in the NS3-NS5B regions of 1B-4, 1B-5, and KAH5 strains showed differences of 6.5%, 8.6%, and 6.1%, respectively, from those of the O strain. Similarly, the amino acid sequences in the NS3–NS5B regions of 1B-4, 1B-5, and KAH5 strains showed differences of 2.6%, 4.7%, and 2.5%, respectively, from those of the O strain. Phylogenetic analysis revealed that O, 1B-4, and KAH5 strains formed the cluster different from 1B-5 strain (Supplemental Fig. 3). These data indicate that sKAH5R and s1B-4R are at a similar genetic distance from the O strain. These two replicons were also found to possess similar features in terms of HCV RNA expression levels and sensitivity to IFN-α. Therefore, sKAH5R and s1B-4R are expected to be useful tools for comparative analyses of anti-HCV determining factors of HCV, especially as regards IFN-λ and statins.

In conclusion, we established an HCV replicon reporter assay system with four different genotype 1b HCV strains. This replicon system is a useful tool for investigating differences in sensitivity to anti-HCV reagents among genotype 1b HCV strains, and it is expected to increase the rate of resolution of HCV cases otherwise resistant to current IFN therapy.

Acknowledgements

The authors would like to thank Atsumi Morishita and Takashi Nakamura for their technical assistance. This work was supported by grants-in-aid for a third-term comprehensive 10-year strategy for cancer control and for research on hepatitis from the Ministry of Health, Labor, and Welfare of Japan.

Appendix A. Supplementary data

Supplementary data associated with this article can be found, in the online version, at doi:10.1016/j.antiviral.2009.01.007.

References

Blight, K.J., McKeating, J.A., Marcotrigiano, J., Rice, C.M., 2003. Efficient replication of hepatitis C virus genotype 1a RNAs in cell culture. J. Virol. 77, 3181–3190.

Doyle, S.E., Schreckhise, H., Khuu-Duong, K., Henderson, K., Rosler, R., Storey, H., Yao, L., Liu, H., Barahmand-pour, F., Sivakumar, P., Chan, C., Birks, C., Foster, D., Clegg, C.H., Wietzke-Braun, P., Mihm, S., Klucher, K.M., 2006. Interleukin-29 uses a type 1 interferon-like program to promote antiviral responses in human hepatocytes. Hepatology 44, 896–906.

Firpi, R.J., Nelson, D.R., 2007. Current and future hepatitis C therapies. Arch. Med. Res. 38, 678–690.

Ikeda, M., Abe, K., Dansako, H., Nakamura, T., Naka, K., Kato, N., 2005. Efficient replication of a full-length hepatitis C virus genome, strain O, in cell culture, and development of a luciferase reporter system. Biochem. Biophys. Res. Commun. 329, 1350–1359.

Ikeda, M., Abe, K., Yamada, M., Dansako, H., Naka, K., Kato, N., 2006. Different anti-HCV profiles of statins and their potential for combination therapy with interferon. Hepatology 44, 117–125.

Ikeda, M., Kato, N., 2007. Life style-related diseases of the digestive system: cell culture system for the screening of anti-hepatitis C virus (HCV) reagents: suppression of HCV replication by statins and synergistic action with interferon. J. Pharmacol. Sci. 105, 145–150.

Ikeda, M., Kato, N., Mizutani, T., Sugiyama, K., Tanaka, K., Shimotohno, K., 1997. Analysis of the cell tropism of HCV by using in vitro HCV-infected human lymphocytes and hepatocytes. J. Hepatol. 27, 445–454.

Ikeda, M., Yi, M., Li, K., Lemon, S.M., 2002. Selectable subgenomic and genome-length dicistronic RNAs derived from an infectious molecular clone of the HCV-N strain of hepatitis C virus replicate efficiently in cultured Huh7 cells. J. Virol. 76, 2997–3006.

Inoue, K., Umehara, T., Ruegg, U.T., Yasui, F., Watanabe, T., Yasuda, H., Dumont, J.M., Scalfaro, P., Yoshiba, M., Kohara, M., 2007. Evaluation of a cyclophilin inhibitor in hepatitis C virus-infected chimeric mice in vivo. Hepatology 45, 921–928.

Kapadia, S.B., Chisari, F.V., 2005. Hepatitis C virus RNA replication is regulated by host geranylgeranylation and fatty acids. Proc. Natl. Acad. Sci. U.S.A. 102, 2561–2566.

Kato, N., 2001. Molecular virology of hepatitis C virus. Acta Med. Okayama 55, 133–159.

Kato, N., Hijikata, M., Ootsuyama, Y., Nakagawa, M., Ohkoshi, S., Sugimura, T., Shimotohno, K., 1990. Molecular cloning of the human hepatitis C virus genome from Japanese patients with non-A, non-B hepatitis. Proc. Natl. Acad. Sci. U.S.A. 87, 9524–9528.

Kato, N., Sugiyama, K., Namba, K., Dansako, H., Nakamura, T., Takami, M., Naka, K., Nozaki, A., Shimotohno, K., 2003a. Establishment of a hepatitis C virus subgenomic replicon derived from human hepatocytes infected in vitro. Biochem. Biophys. Res. Commun. 306, 756–766.

Kato, T., Date, T., Miyamoto, M., Furusaka, A., Tokushige, K., Mizokami, M., Wakita, T., 2003b. Efficient replication of the genotype 2a hepatitis C virus subgenomic replicon. Gastroenterology 125, 1808–1817.

Kishine, H., Sugiyama, K., Hijikata, M., Kato, N., Takahashi, H., Noshi, T., Nio, Y., Hosaka, M., Miyanari, Y., Shimotohno, K., 2002. Subgenomic replicon derived from a cell line infected with the hepatitis C virus. Biochem. Biophys. Res. Commun. 293, 993–999.

Lohmann, V., Korner, F., Koch, J., Herian, U., Theilmann, L., Bartenschlager, R., 1999. Replication of subgenomic hepatitis C virus RNAs in a hepatoma cell line. Science 285, 110–113.

Marcello, T., Grakoui, A., Barba-Spaeth, G., Machlin, E.S., Kotenko, S.V., MacDonald, M.R., Rice, C.M., 2006. Interferons alpha and lambda inhibit hepatitis C virus replication with distinct signal transduction and gene regulation kinetics. Gastroenterology 131, 1887–1898.

Mori, K., Abe, K., Dansako, H., Ariumi, Y., Ikeda, M., Kato, N., 2008. New efficient replication system with hepatitis C virus genome derived from a patient with acute hepatitis C. Biochem. Biophys. Res. Commun. 371, 104–109.

Nakagawa, M., Sakamoto, N., Tanabe, Y., Koyama, T., Itsui, Y., Takeda, Y., Chen, C.H., Kakinuma, S., Oooka, S., Maekawa, S., Enomoto, N., Watanabe, M., 2005. Suppression of hepatitis C virus replication by cyclosporin a is mediated by blockade of cyclophilins. Gastroenterology 129, 1031–1041.

Pagliaccetti, N.E., Eduardo, R., Kleinstein, S.H., Mu, X.J., Bandi, P., Robek, M.D., 2008. Interleukin-29 functions cooperatively with interferon to induce antiviral gene expression and inhibit hepatitis C virus replication. J. Biol. Chem. 283, 30079–30089.

Pietschmann, T., Lohmann, V., Kaul, A., Krieger, N., Rinck, G., Rutter, G., Strand, D., Bartenschlager, R., 2002. Persistent and transient replication of full-length hepatitis C virus genomes in cell culture. J. Virol. 76, 4008–4021.

Robek, M.D., Boyd, B.S., Chisari, F.V., 2005. Lambda interferon inhibits hepatitis B and C virus replication. J. Virol. 79, 3851–3854.

Tanaka, T., Kato, N., Cho, M.J., Sugiyama, K., Shimotohno, K., 1996. Structure of the 3′ terminus of the hepatitis C virus genome. J. Virol. 70, 3307–3312.

Taylor, D.R., Shi, S.T., Romano, P.R., Barber, G.N., Lai, M.M.C., 1999. Inhibition of the interferon-inducible protein kinase PKR by HCV E2 protein. Science 285, 107–109.

Uze, G., Monneron, D., 2007. IL-28 and IL-29: newcomers to the interferon family. Biochimie 89, 729–734.

Wang, C., Gale Jr., M., Keller, B.C., Huang, H., Brown, M.S., Goldstein, J.L., Ye, J., 2005. Identification of FBL2 as a geranylgeranylated cellular protein required for hepatitis C virus RNA replication. Mol. Cell 18, 425–434.

Watashi, K., Hijikata, M., Hosaka, M., Yamaji, M., Shimotohno, K., 2003. Cyclosporin A suppresses replication of hepatitis C virus genome in cultured hepatocytes. Hepatology 38, 1282–1288.

Ye, J., Wang, C., Sumpter Jr., R., Brown, M.S., Goldstein, J.L., Gale Jr., M., 2003. Disruption of hepatitis C virus RNA replication through inhibition of host protein geranylgeranylation. Proc. Natl. Acad. Sci. U.S.A. 100, 15865–15870.

ELSEVIER

Journal of Hepatology 50 (2009) 883–894

Journal of Hepatology

www.elsevier.com/locate/jhep

HCV replication suppresses cellular glucose uptake through down-regulation of cell surface expression of glucose transporters☆

Daisuke Kasai[1,†], Tetsuya Adachi[1,†], Lin Deng[1], Motoko Nagano-Fujii[1], Kiyonao Sada[1], Masanori Ikeda[2], Nobuyuki Kato[2], Yoshi-Hiro Ide[1], Ikuo Shoji[1], Hak Hotta[1,*]

[1]*Divisions of Microbiology, Kobe University Graduate School of Medicine, 7-5-1 Kusunoki-cho, Chuo-ku, Kobe 650-0017, Japan*
[2]*Department of Molecular Biology, Okayama University Graduate School of Medicine and Dentistry, Okayama, Japan*

See Editorial, pages 845–847

***Background/Aims*: Persistent infection with hepatitis C virus (HCV) causes extrahepatic diseases, including diabetes. We investigated the possible effect(s) of HCV replication on cellular glucose uptake and expression of the facilitative glucose transporter (GLUT) 2 and 1.**

***Methods*: We used Huh-7.5 cells harboring either an HCV subgenomic RNA replicon (SGR) or an HCV full-genomic RNA replicon (FGR), HCV-infected cells, and the respective cells treated with interferon (IFN). We also used liver tissue samples obtained from patients with or without HCV infection.**

***Results*: Glucose uptake and surface expression of GLUT2 and GLUT1 were suppressed in SGR, FGR and HCV-infected cells compared to the control cells. Expression levels of GLUT2 mRNA, but not GLUT1 mRNA, were lower in SGR, FGR and HCV-infected cells than in the control. Luciferase reporter assay demonstrated decreased GLUT2 promoter activities in SGR, FGR and HCV-infected cells. IFN treatment restored glucose uptake, GLUT2 surface expression, GLUT2 mRNA expression and GLUT2 promoter activities. Also, GLUT2 expression was reduced in hepatocytes of liver tissues obtained from HCV-infected patients.**

***Conclusions*: HCV replication down-regulates cell surface expression of GLUT2 partly at the transcriptional level, and possibly at the intracellular trafficking level as suggested for GLUT1, thereby lowering glucose uptake by hepatocytes.**

***Keywords*: Diabetes mellitus; Down-regulation; Glucose uptake; GLUT1; GLUT2; Hepatitis C virus; Hepatocyte; Interferon; Replicon**

1. Introduction

Hepatitis C virus (HCV) is a small, enveloped RNA virus, which belongs to the genus *Hepacivirus* within the family *Flaviviridae*. The viral genome consists of single-stranded, positive-sense RNA of 9.6 kb that encodes a polyprotein of about 3000 amino acids. There are six major genotypes of HCV worldwide, with each genotype being further classified into a number of subtypes, such as HCV-1a and -1b [1,2]. The polyprotein is processed by host cellular and viral proteases to yield at least 10 structural and nonstructural (NS) proteins, such

Received 15 June 2008; received in revised form 19 November 2008; accepted 11 December 2008; available online 27 February 2009
Associate Editor: F. Zoulim

☆ The authors who have taken part in the research of this manuscript declared that they do not have a relationship with the manufacturers of the materials involved either in the past or present and they did not receive funding from the manufacturers to carry out their research.

* Corresponding author. Tel.: +81 78 3825500; fax: +81 78 3825519.
E-mail address: hotta@kobe-u.ac.jp (H. Hotta).
† These authors contributed equally to this work.

Abbreviations: FGR, full-genome RNA replicon; GLUT, glucose transporter; HBV, hepatitis B virus; HCV, hepatitis C virus; IFN, interferon; SGR, subgenomic RNA replicon.

0168-8278/$36.00
doi:10.1016/j.jhep.2008.12.029

as core protein, envelope glycoproteins (E1 and E2), p7, NS2, NS3, NS4A, NS4B, NS5A and NS5B [3,4].

HCV prevails in most parts of the world with an estimated number of about 170 million carriers and, hence, HCV infection is a major global healthcare problem [5]. Persistent infection with HCV causes not only liver diseases, including hepatitis, but also extrahepatic manifestations, such as type 2 diabetes [6–8]. While it has been known that liver cirrhosis impairs the glucose metabolism of the liver, there are some reports showing that HCV-infected patients over 40 years old have an increased risk for type 2 diabetes – three times higher than that for patients without HCV infection [9,10]. These reports imply the possibility that HCV infection directly predisposes the host towards type 2 diabetes. However, the precise mechanism(s) is poorly understood.

Glucose is transported into the cell via various isoforms of the facilitative glucose transporter (GLUT) that are present in most cells. Currently, a total of 14 isoforms have been identified in the GLUT family [11–13]. GLUT2 is expressed tissue-specifically in the liver, pancreatic β-cells, hypothalamic glial cells, retina and enterocytes [14]. On the other hand, GLUT1 is expressed at high levels in all fetal tissues and, in adults, it is widely expressed but most abundant in erythrocytes, endothelial cells of the blood–brain barrier, renal tubules of the kidney, and any kind of malignant cells including hepatocellular carcinoma [13].

In the present study, we demonstrated that HCV infection suppressed hepatocytic glucose uptake through down-regulation of surface expression of GLUT in a human hepatocellular carcinoma-derived cell line Huh-7.5. We also demonstrated that GLUT2 expression in hepatocytes of the liver tissues from HCV-infected patients was lower than in those from patients without HCV infection. We propose that HCV replication decreases glucose uptake and cell surface expression of GLUT, which would eventually lead to glucose metabolism disorder.

2. Materials and methods

2.1. Cell culture, HCV RNA replication, HCV infection and IFN treatment

A human hepatoma-derived cell line, Huh-7.5, which is highly permissive to HCV RNA replication [15], was kindly provided by Dr. C.M. Rice (The Rockefeller University, New York, NY, USA). The cells were maintained in Dulbecco's modified Eagle's medium supplemented with 10% heat-inactivated fetal calf serum.

Huh-7.5 cells stably harboring an HCV-1b subgenomic RNA replicon (referred to as SGR cells, hereafter) were prepared as describe previously [16–18], using pFK5B/2884Gly (a kind gift from Dr. R. Bartenschlager, University of Heidelberg, Heidelberg, Germany). In SGR cells, the HCV subgenomic RNA replicon autonomously replicates to express NS3 to NS5B of HCV (Fig. 1). Cells harboring a full-length HCV-1b RNA replicon derived from pON/C-5B (referred to as FGR cells, hereafter) were described previously [19,20]. In FGR cells, the genome-size HCV RNA replicon autonomously replicates to express all the HCV proteins (the core protein, E1, E2, p7, NS2, NS3 to NS5B).

The pFL-J6/JFH1 plasmid that encodes the entire viral genome of a chimeric strain of HCV-2a, J6/JFH1 [21], was kindly provided by Dr. C.M. Rice. The HCV RNA genome was transcribed *in vitro* from pFL-J6/JFH1 and transfected to Huh-7.5 cells. The virus produced in the culture supernatant was used for infection experiments at multiplicities of infection of 1.0 and cultured for 5 days after virus infection.

In some experiments, SGR and FGR cells, as well as HCV-infected cells at 5 days after virus infection, were treated with 1000 IU/ml of IFN (Sigma, St. Louis, MI, USA) for 10 days to eliminate HCV replication.

2.2. Immunofluorescence

Cells were fixed with 3.7% paraformaldehyde and incubated with mouse monoclonal antibody against HCV NS5A (Chemicon International, Inc., Temecula, CA, USA) or HCV core (Abcam, Tokyo, Japan). The cells were then incubated with fluorescein isothiocyanate (FITC)-conjugated goat anti-mouse IgG (MBL Co. Ltd., Nagoya, Japan), and observed under a fluorescent microscope (BX51; Olympus, Tokyo, Japan).

2.3. Immunoblotting

Cells were solubilized in lysis buffer as reported previously [22]. The cell lysates were electrophoresed subjected to 8% polyacrylamide gel electrophoresis and transferred to polyvinylidene difluoride membrane (Millipore Corp., Billerica, MA, USA). The membranes were incubated with mouse monoclonal antibodies against HCV NS5A or NS3 (Chemicon), followed by incubation with peroxidase-conjugated goat anti-mouse IgG (MBL). The positive bands were visualized by using ECL detection system (GE Healthcare UK Ltd., Buckinghamshire, UK).

2.4. Uptake of 2-deoxy-D-glucose and thymidine

Cells cultured in 12-well plates were deprived of serum by incubation in serum-free medium for 12 h. The cells were then pre-incubated for 20 min in 450 μl of KRH (25 mM Hepes, 120 mM NaCl, 5 mM KCl, 1.2 mM $MgSO_4$, 1.3 mM $CaCl_2$, 1.3 mM KH_2PO_4 and 0.1% BSA, pH 7.4). Glucose uptake assay was performed as describe previously [23]. In brief, glucose uptake was initiated by addition of 50 μl of reaction solution (KRH containing 0.5 mM, 0.25 μCi 2-deoxy-D-[1,2-^{3}H]glucose) to each well. As a negative control, 100 μM phloretin was added to reaction solution. After 10 min, transport was terminated by washing the cells with ice-cold KRH buffer containing 100 μM phloretin. The cells were solubilized by 0.1% sodium dodecyl sulfate, and the incorporated radioactivity was measured by liquid scintillation counter (LS6500; Beckman Coulter, Fullerton, CA). In some experiments, GLUT1 and GLUT2 were ectopically expressed by using the pCAGGS expression vector [24] and glucose uptake was measured as described above.

2.5. Flow cytometry

To examine cell surface expression of GLUT1 and GLUT2, cells harvested in PBS containing 0.2% EDTA were incubated with rabbit polyclonal antibodies against GLUT1 or GLUT2 (1:200; Alpha Diagnostic International, San Antonio, TX, USA) on ice for 1 h. After being washed, the cells were incubated with FITC-labeled goat anti-rabbit IgG (1:200; BD Pharmingen, Franklin Lakes, NJ, USA) on ice for another 1 h. Analysis was carried out using flow cytometer and a total of 10,000 live cell events were measured. Results were displayed graphically as overlaying histograms demonstrating the shift of the mean FITC staining value.

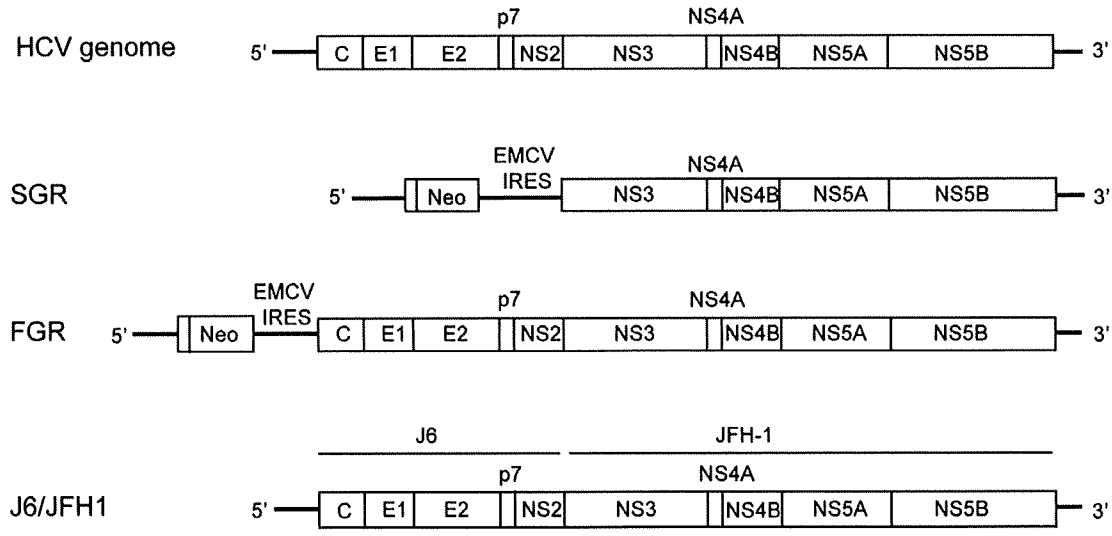

Fig. 1. The HCV genome and HCV RNA replicons. Schematic diagram of the HCV genome, SGR, FGR and the chimeric HCV J6/JFH1 genome are shown. EMCV IRES, encephalomyocarditis virus internal ribosome entry site; Neo, neomycin-resistance gene.

2.6. Real-time quantitative RT-PCR

Total cellular RNA was isolated using the TRIzol reagent (Invitrogen Corp., Carlsbad, CA, USA) and cDNA was generated using QuantiTect Reverse Transcription system (Qiagen, Valencia, CA, USA). Real-time quantitative PCR was performed on a SYBR *Premix Ex Taq* (Takara Bio, Kyoto, Japan) using SYBR green chemistry in ABI PRISM 7000 (Applied Biosystems, Foster, CA, USA). β-Glucuronidase was used as an internal control. The primers used are shown in Table 1.

2.7. Luciferase reporter assay

We constructed the human GLUT2 promoter-luciferase reporter gene (pGLUT2-1291Luc) by cloning a 1.6-kb genomic fragment that encompasses the human GLUT2 promoter (−1291 to +308) [14] into the pGL4 vector plasmid (Promega, Madison, WI, USA). pGLUT2-1291Luc thus contains a 1291-bp fragment of the human GLUT2 promoter upstream of the minimal promoter and the coding sequence of the *Photinus pyralis* (firefly) luciferase. pRL-CMV-*Renilla* (Promega) was used as an internal control. Cells were transfected with pGLUT2-1291Luc (1 μg) and pRL-CMV-*Renilla* (10 ng). After 24 h, a luciferase assay was performed by using Dual-luciferase reporter assay system (Promega). Firefly and *Renilla* luciferase activities were measured by Lumat LB 9501 (Berthold, Bad Wildbad, Germany). Firefly luciferase activity was normalized to *Renilla* luciferase activity for each sample.

2.8. Immunohistochemistry

Human adult liver autopsy materials and surgically removed liver tissues of patients with HCV- or HBV-associated hepatocellular carcinoma, and those with metastatic liver cancer were obtained with written informed consent. The tissues were fixed with 10% buffered formalin (pH 7.0), embedded in paraffin and sectioned at intervals of 4 μm. Immunohistochemical staining was performed with a DAKO ENVISION+ Kit (Dako, Glostrup, Denmark). In brief, fixed sections were treated with 3% hydrogen peroxide, and were autoclaved at 121 °C for 20 min. Then, the sections were incubated with a blocking solution and then with either anti-GLUT2 rabbit polyclonal antibody (Santa Cruz Biotechnology, Santa Cruz, CA, USA) or normal rabbit IgG (Santa Cruz Biotechnology) as a control. The sections were incubated with horseradish peroxidase-labeled polymer-conjugated goat anti-rabbit IgG, followed by incubation in a chromogenic solution. The sections were then counterstained with hematoxylin and examined with a light microscope. GLUT2 expression levels were arbitrarily determined by two examiners, including a pathologist, in a blinded manner.

2.9. Statistical analysis

Results were expressed as mean ± SEM. Statistical significance was evaluated by ANOVA, and statistical significance was defined as $P < 0.05$.

Table 1
Sequences and positions of the primers used in this study.

Gene name (GenBank ID)	Primer	Position	PCR product (bp)
GLUT2	5′-TGGGCTGAGGAAGAGACTGT-3′	279–298	461
(J03810)	5′-AGAGACTGAAGGATGGCTCG-3′	739–720	
GLUT1	5′-TGAACCTGCTGGCCTTC-3′	437–453	399
(AK292791)	5′-GCAGCTTCTTTAGCACA-3′	835–819	
HCV NS5B	5′-ACCAAGCTCAAACTCACTCCA-3′	9191–9211	119
(AJ238799)	5′-AGCGGGGTCGGGCACGAGACA-3′	9309–9289	
β-glucuronidase	5′-ATCAAAAACGCAGAAAATACG-3′	1747–1767	238
(M15182)	5′-ACGCAGGTGGTATCAGTCTTG-3′	1984–1964	

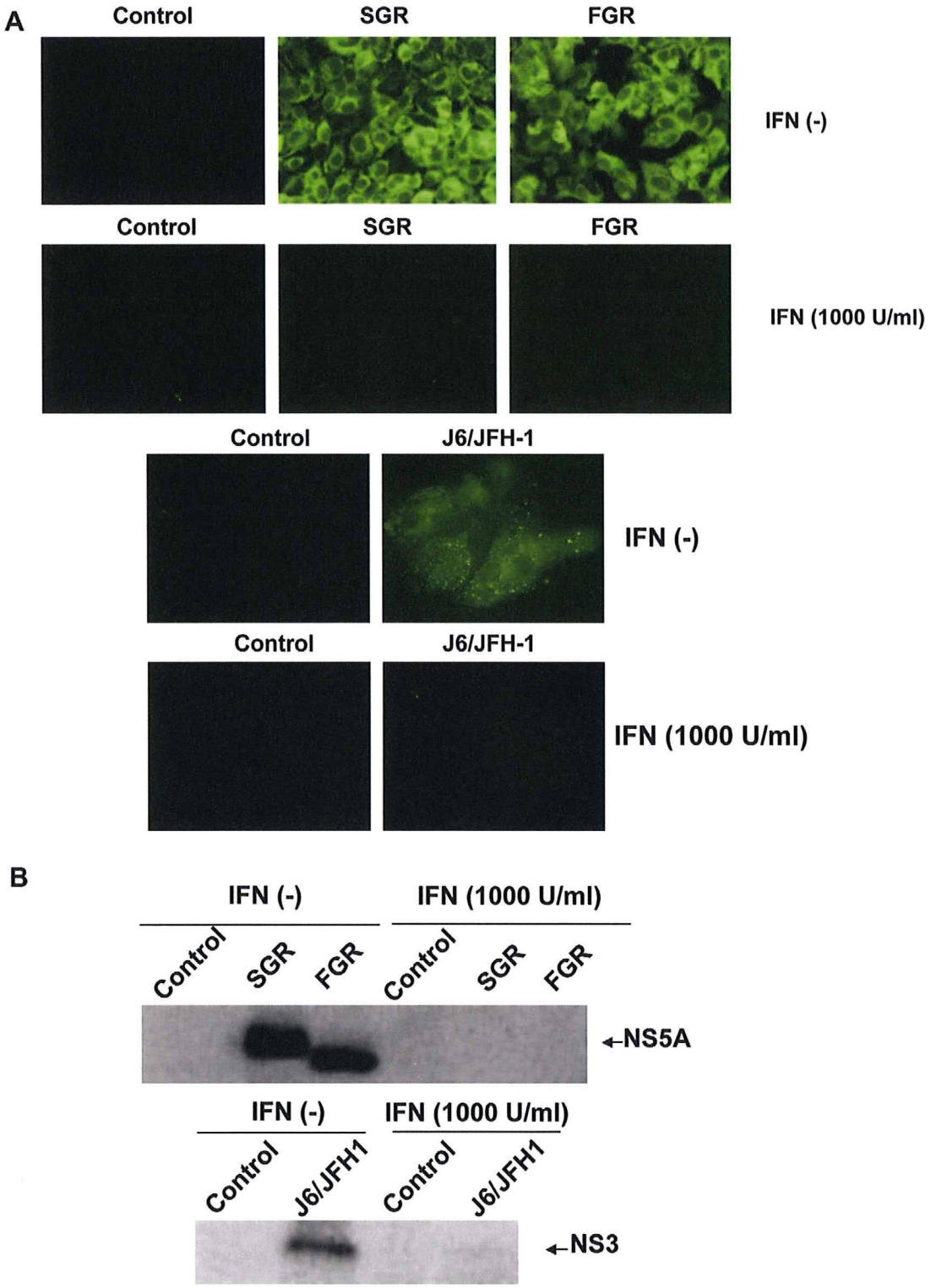

Fig. 2. Expression of HCV proteins in SGR, FGR, HCV-infected cells and the respective cells treated with IFN. (A) Cells were immunostained with anti-NS5A antibody (for SGR, FGR and the control cells) or anti-core antibody (for HCV-infected cells and the control). In parallel, cells were treated with IFN (1000 IU/ml) for 10 days to eliminate HCV replication before being subjected to immunostaining. (B) Cells were analyzed by immunoblotting with anti-NS5A antibody (upper panel) or anti-NS3 antibody (lower panel). In parallel, cells were treated with IFN (1,000 IU/ml) for 10 days to eliminate HCV replication before being subjected to immunoblotting.

3. Results

3.1. HCV protein expression in SGR, FGR, HCV-infected cells and those treated with IFN

Immunofluorescence analysis revealed that almost all the cells in SGR and FGR cultures, and >90% of the cells in the HCV J6/JFH1-infected culture were positive for HCV antigens (Fig. 2A). Western blot analysis also confirmed HCV protein expression in SGR, FGR and HCV-infected cells (Fig. 2B). In some experiments, HCV replication in SGR, FGR and HCV-infected cells was eliminated by IFN treatment for 10 days (Fig. 2A and B).

3.2. Selective suppression of cellular glucose uptake by HCV replication

2-Deoxygluose uptake levels in SGR, FGR and HCV-infected cells were significantly suppressed by about 50–60%, compared with the control Huh-7.5 cells (Fig. 3A and B). On the other hand, thymidine uptake, which was used as a control, did not significantly differ among all the cells tested (data not shown). Moreover, glucose uptake levels in SGR, FGR and HCV-infected cells were restored by IFN treatment (Fig. 3A and B). These results strongly suggest that cellular glucose uptake is selectively suppressed by HCV RNA replication.

3.3. Down-regulation of cell surface expression of GLUT2 and GLUT1 by HCV replication

GLUT2 is the principal glucose transporter of hepatocytes *in vivo* while GLUT1 is expressed in a wide variety of cultured cells. We therefore examined cell surface expression of GLUT2 and GLUT1 by flow cytometry analysis. As shown in Fig. 4A, cell surface expression of GLUT2 and GLUT1 was markedly down-regulated in SGR and FGR cells, compared with the control. On the other hand, cell surface expression of transferrin receptor was not significantly suppressed in SGR or FGR, compared with the control, with the result ensuring the specificity of the down-regulation of GLUT2 and GLUT1 cell surface expression in SGR and FGR (Fig. 4A). Moreover, treatment of SGR and FGR cells with IFN restored the surface expression of GLUT2 and GLUT1 (Fig. 4A). These results suggest that HCV RNA replication specifically mediates down-regulation of GLUT2 and GLUT1.

Down-regulation of GLUT2 surface expression was observed also in HCV-infected cells (Fig. 4B). On the other hand, down-regulation of GLUT1 surface expression was only marginal and, compared to that of GLUT2, less evidently observed in HCV-infected cells. As a control, cell surface expression of transferrin receptor did not differ at all between HCV-infected cells and the control. Again, treatment of HCV-infected cells with IFN restored surface expression of GLUT2 (Fig. 4B).

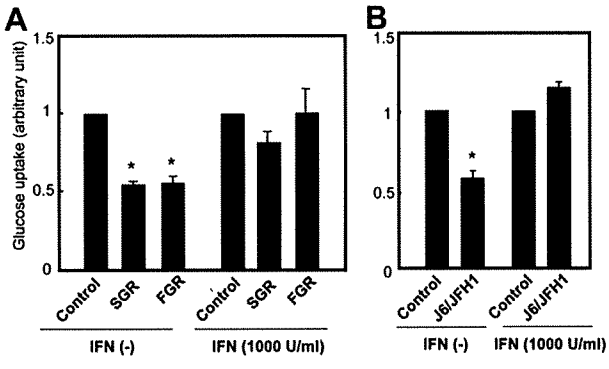

Fig. 3. Selective suppression of cellular glucose uptake by HCV replication. (A) Uptake of 2-deoxy-D-[1,2-^{3}H] glucose in SGR, FGR and HCV-negative control. In parallel, cells were treated with IFN (1000 IU/ml) for 10 days to eliminate HCV replication before being subjected to glucose uptake analysis. Data represent mean ± SEM of four independent experiments and the values for the control cells were arbitrarily expressed as 1.0. $^*P < 0.01$, compared with the control. (B) Uptake of 2-deoxy-D-[1,2-^{3}H] glucose in J6/JFH-1-infected cells and the uninfected control. In parallel, cells at 5 days after infection were treated with IFN (1000 IU/ml) for 10 days to eliminate HCV replication before being subjected to glucose uptake analysis.

3.4. Proteasomal degradation is not involved in the down-regulation of GLUT2 or GLUT1

Some viruses down-regulate cell surface molecules, such as immunoreceptors and intercellular adhesion molecules, through ubiquitination and proteasomal degradation of the target proteins [25]. To test this possibility, we treated SGR and FGR cells with lactacystin, a potent proteasome inhibitor. While lactacystin treatment enhanced cell surface expression of transferrin receptor, the same treatment did not increase cell surface expression of GLUT2 or GLUT1 in SGR or FGR cells (Fig. 5). This result suggested that down-regulation of cell surface expression of GLUT2 or GLUT1 in HCV-replicating cells was not due to increased degradation through the ubiquitin–proteasome system. The result rather implied the possible involvement of another mechanism(s), e.g., transcriptional suppression and/or impaired intracellular trafficking.

3.5. Transcriptional suppression of GLUT2, but not GLUT1, by HCV replication

To examine whether HCV RNA replication suppresses GLUT2 and GLUT1 expression at the transcriptional level, we measured mRNA expression levels by quantitative RT-PCR. The results obtained revealed that GLUT2 mRNA levels were reduced significantly in SGR, FGR and HCV-infected cells, compared to the control (Fig. 6A). It should be noted that the degree of GLUT2 mRNA suppression was greater in FGR

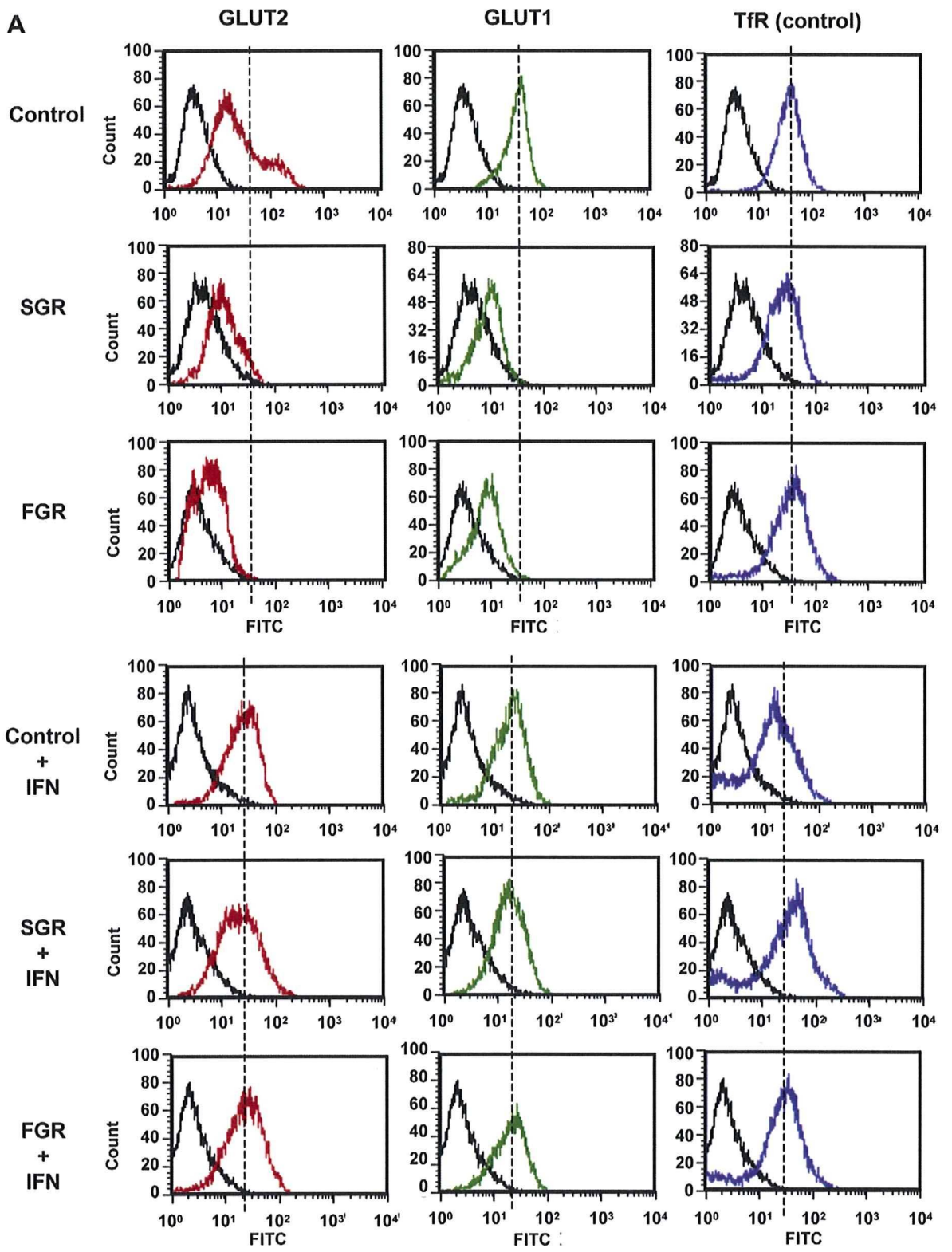

Fig. 4. Down-regulation of cell surface expressions of GLUT2 and GLUT1 by HCV replication. (A) SGR, FGR, the HCV-negative control cells were stained with specific antibodies, followed by FITC-conjugated second antibody (GLUT2, red line; GLUT1, green line) or stained with FITC-conjugated antibody alone (black line). Transferrin receptor (TfR) served as a control (blue line). In parallel, cells were treated with IFN (1000 IU/ml) for 10 days to eliminate HCV replication before being subjected to flow cytometry. (B) HCV-infected cells and the uninfected control were analyzed by flow cytometry as in (A). In parallel, cells at 5 days after infection were treated with IFN (1000 IU/ml) for 10 days to eliminate HCV replication before being subjected to flow cytometry analysis.

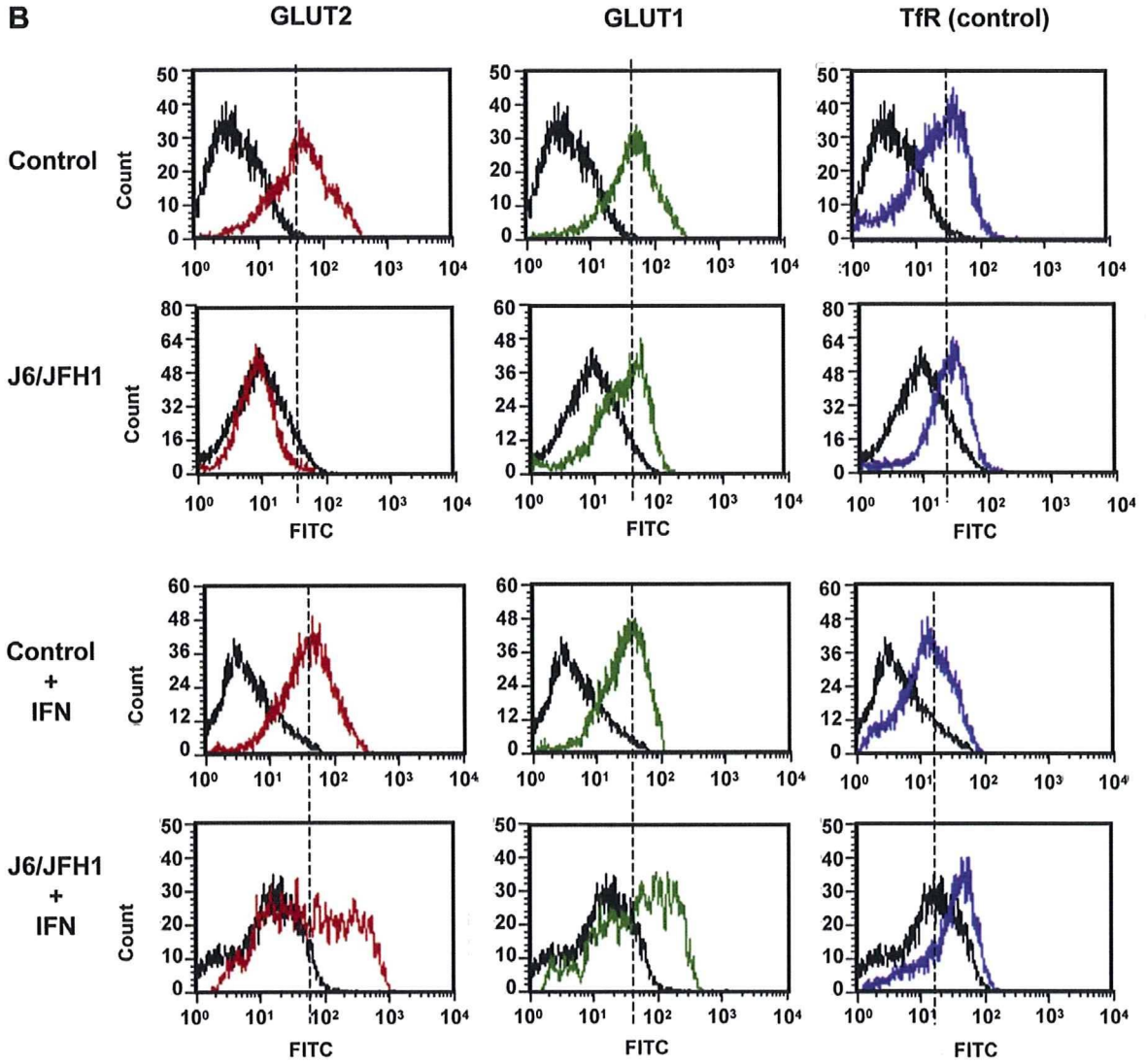

Fig. 4 (*continued*)

than in SGR cells. On the other hand, GLUT1 mRNA levels were not affected by HCV RNA replication (SGR and FGR) or HCV infection (Fig. 6B).

We also confirmed that GLUT2 mRNA expression levels in SGR, FGR and HCV-infected cells were restored by IFN treatment (Fig. 6A).

3.6. Suppression of GLUT2 promoter activity by HCV replication

Next, we performed luciferase reporter assay to examine the possible effect of HCV replication on GLUT2 promoter activities. The result obtained demonstrated that GLUT2 promoter activities were significantly suppressed in SGR, FGR and HCV-infected cells, compared to the control cells (Fig. 6C). Furthermore, GLUT2 promoter activities in SGR, FGR and HCV-infected cells were restored by IFN treatment. It is thus likely that HCV replication suppresses GLUT2 promoter activity, thereby decreasing GLUT2 mRNA levels.

3.7. Ectopically expressed GLUT1 or GLUT2 mediates increased glucose uptake in SGR, FGR and HCV-infected cells

We examined the possible effects of ectopically expressed GLUT1 and GLUT2 on glucose uptake in SGR, FGR and HCV-infected cells. Glucose uptake was significantly increased by ectopically expressed GLUT1 or GLUT2 in SGR, FGR and HCV-infected cells as well as in the control Huh-7.5 cells (Fig. 6D). It should be noted that, in this series of transient transfection experiments, only ca. 20% of the cells were ectopically overexpressing GLUT1 or GLUT2. These results collectively suggest the possibility that down-regulation

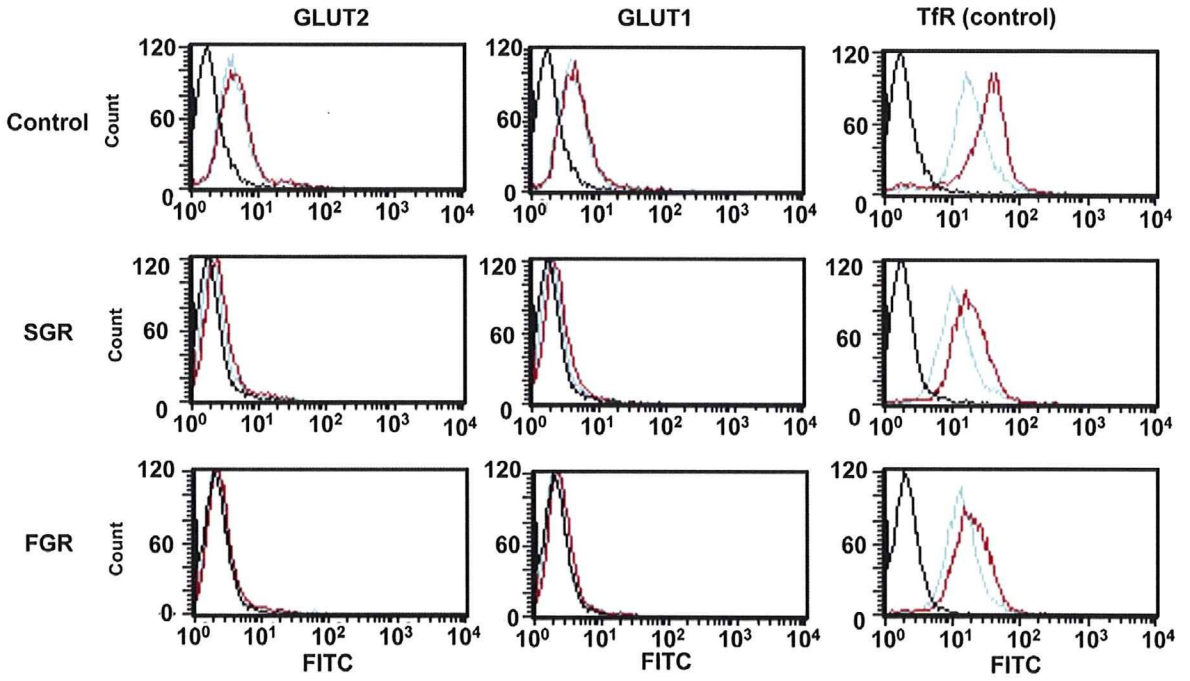

Fig. 5. Effects of lactacystin treatment on cell surface expression of GLUT2, GLUT1 and transferrin receptor (TfR). Cells were treated with lactacystin (10 μM) overnight to inhibit proteasomal degradation, and analyzed by flow cytometry. Cells treated with lactacystin are shown in red line and those left untreated in blue line. The negative controls stained with FITC-conjugated antibody alone are shown in black line.

of GLUT1 and GLUT2 expression is primarily involved in the decreased glucose uptake in SGR, FGR and HCV-infected cells.

3.8. Decreased GLUT2 expression in hepatocytes obtained from HCV-infected patients

GLUT2 is the principal glucose transporter expressed in hepatocytes *in vivo*. As shown in Fig. 7B, practically all hepatocytes obtained from patients without HCV infection showed positive staining for GLUT2, which was most evidently observed near the plasma membrane. On the other hand, hepatocytes obtained from HCV-infected patients showed markedly reduced GLUT2 staining in most, if not the entire, areas of the section, compared with the uninfected control (Fig. 7D). This heterogeneous staining pattern might reflect concomitant presence of areas comprising either virus-infected or uninfected hepatocytes in a tissue sample. Whereas all the sections obtained from 8 patients without HCV infection showed evenly positive staining for GLUT2, sections from 8 (89%) of 9 HCV-infected patients showed moderately to markedly reduced GLUT2 staining (Table 2). Reduced GLUT2 staining was observed also with hepatocytes in the liver tissues obtained from HBV-infected patients. However, the areas of reduced GLUT2 staining appeared to be more restricted in sections obtained from HBV-infected patients than in those from HCV-infected ones.

4. Discussion

HCV infection is known as an initiation and precipitating factor of type 2 diabetes [7–10,26,27]. Progression of liver fibrosis induced by persistent viral infection may induce diabetes [28]. Furthermore, it has been reported that the prevalence of diabetes is higher among patients with HCV-associated liver cirrhosis than in those with HBV-associated cirrhosis [7]. It is likely, therefore, that HCV infection itself is a risk factor of diabetes. Previous reports suggest that HCV infection directly causes insulin resistance that would cause the progression of diabetes [29–31]. However, the underlying mechanism(s) is not yet completely elucidated. In this study, we analyzed the effect of HCV infection on cellular glucose uptake and expression of glucose transporters.

We observed that glucose uptake was suppressed in cells harboring HCV RNA replicons (SGR and FGR) and those infected with HCV than in the control cells (Fig. 3). It has been reported that glucose disposal *in vivo* occurs through both insulin-dependent and insulin-independent mechanism [32]. We observed that treatment of SGR, FGR and the control Huh-7.5 cells with insulin (10^{-4} M to 10^{-9} M) increased glucose uptake by only about 50% from their basal levels (data not shown). Nevertheless, decreased glucose uptake by HCV-infected hepatocytes is a potential cause of hyperglycemia as the liver is a big organ accounting for 2% of the total body weight.

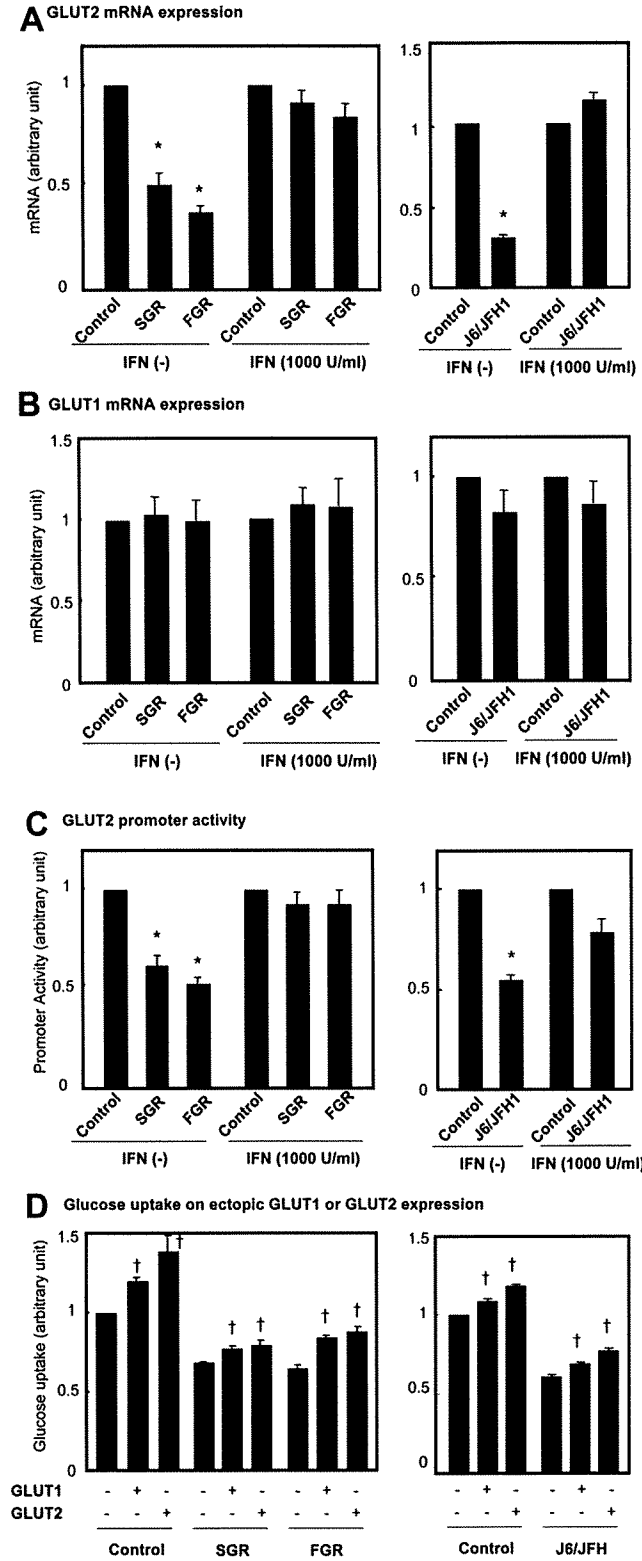

Fig. 6. Differential suppression of GLUT2 and GLUT1 mRNAs by HCV replication. (A and B) Quantitative RT-PCR analysis of mRNA for GLUT2 (A) and GLUT1 (B). mRNA expression levels of GLUT2 and GLUT1 in SGR, FGR and HCV-infected cells were determined and normalized with β-glucuronidase mRNA levels. In parallel, cells were treated with IFN (1000 IU/ml) for 10 days to eliminate HCV replication before being subjected to quantitative RT-PCR analysis. Data represent mean ± SEM of three independent experiments. $^{*}P < 0.01$, compared with the control. (C) GLUT2 promoter activities in SGR and FGR, HCV-infected cells were analyzed using luciferase reporter assay. In parallel, cells were treated with IFN (1000 IU/ml) for 10 days to eliminate HCV replication before being subjected to luciferase reporter assay. Data represent mean ± SEM of five independent experiments. $^{*}P < 0.01$, compared with the control. (D) Glucose uptake in cells ectopically expressing GLUT1 or GLUT2. Data represent mean ± SEM of two independent experiments. $^{\dagger}P < 0.01$, compared with mock transfected control.

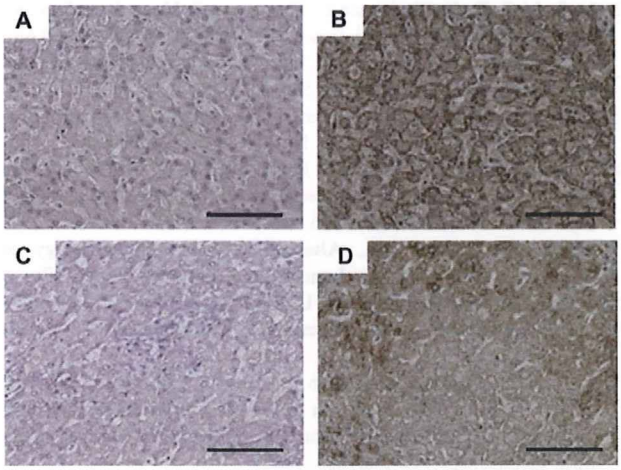

Fig. 7. Down-regulation of GLUT2 expression in HCV-infected human liver tissues *in vivo*. Normal human adult liver tissues (A and B) and HCV-infected, non-cancerous liver tissues (C and D) were fixed with formalin, sectioned and stained with normal rabbit IgG (A and C) or polyclonal anti-GLUT2 antibody (B and D). Scale bar = 100 μm.

Any proliferating cell requires energy sources, including glucose, and GLUTs play an important role in glucose uptake into the cell. In the liver, GLUT2 is the predominant glucose transporter, which regulates glucose metabolism by mediating a bidirectional transport, both entry and exit, of glucose into and from hepatocytes [13]. GLUT1, on the other hand, is known to be expressed in malignant cells including hepatocellular carcinoma [12,13] and a wide variety of cultured cells. In the present study we found that cell surface expression of GLUT2 and GLUT1 was markedly suppressed in SGR, FGR and HCV-infected cells compared to the control (Fig. 4A and B).

Table 2
Reduction of GLUT2 expression in hepatocytes of HCV-infected and HBV-infected human liver tissues.

Liver tissues	Sample No.	Reduction of GLUT2 expression
Uninfected	1	– *
	2	–
	3	–
	4	–
	5	–
	6	–
	7	–
	8	–
HCV-infected	9	1+ (Focal)[a]
	10	1+ (Focal)
	11	3+ (Diffuse)
	12	3+ (Diffuse)
	13	3+ (Diffuse)
	14	3+ (Focal)
	15	–
	16	2+ (Focal)
	17	3+ (Diffuse)
HBV-infected	18	–
	19	3+ (Diffuse)
	20	1+ (Focal)
	21	–
	22	2+ (Focal)
	23	1+ (Focal)
	24	2+ (Focal)

* -, no reduction; 1+, weak reduction; 2+, moderate reduction; 3+, strong reduction.

[a] Parentheses indicate either focal or diffuse appearance of the areas with reduced GLUT2 expression in each liver tissue sample.

GLUT2 expression is regulated at the transcriptional level, at least partly, by glucose [33]. It has been reported that hyperglycemia increases the GLUT2 mRNA and protein expression in an *in vivo* study [34]. Our present study demonstrated that GLUT2 mRNA expression was significantly suppressed in SGR, FGR and HCV-infected cells compared to the control (Fig. 6A). Consistent with this result, GLUT2 promoter activities, as measured by luciferase reporter assay, were suppressed in SGR, FGR and HCV-infected cells (Fig. 6C). In this connection, it was reported that GLUT2 promoter activities were up-regulated by sterol response element-binding protein (SREBP)-1c [35,36]. We confirmed in our study that GLUT2 promoter activities were up-regulated by over-expression of human SREBP-1c, and that the SREBP-1c-mediated GLUT2 promoter activities were suppressed significantly in SGR, FGR and HCV-infected cells (data not shown).

Unlike GLUT2 mRNA, GLUT1 mRNA was not suppressed by HCV RNA replication or HCV infection (Fig. 6B). Nevertheless, cell surface expression of GLUT1 was markedly down-regulated in SGR and FGR cells (Fig. 4A). As GLUT1 surface expression was not restored by treatment with lactacystin, a potent proteasome inhibitor (Fig. 5), it was unlikely that HCV-mediated suppression of GLUT1 surface expression was mediated through increased degradation by the ubiquitin-proteasome system. We assume that intracellular trafficking of GLUT1 (and possibly GLUT2 as well) is impaired by HCV RNA replication although we could not precisely prove it due mainly to the lack of an appropriate antibody that enables us to monitor GLUT1 trafficking. Further study is needed to elucidate the issue.

By means of immunohistochemical analysis, we confirmed that GLUT2 was strongly expressed in hepatocytes of the liver tissues obtained from all of 8 individuals without HCV infection (Fig. 7B and Table 2). More importantly, we demonstrated that GLUT2 expression was significantly down-regulated in hepatocytes obtained from 8 of 9 HCV-infected patients (Fig. 7D and Table 2). Interestingly, the areas where GLUT2 down-regulation was observed appeared to be scattered across the liver tissue sections. This may reflect the general observation that a group of hepatocytes in limited areas of the hepatic lobules, but not all the hepatocytes, are infected with HCV *in vivo*. By means of real-time quantitative PCR analysis, we found a tendency that levels of GLUT2 mRNA expression in liver tissues obtained from HCV-infected patients were lower than that obtained from uninfected controls although the dif-

ference was not statistically significant (data not shown). As stated above, not all the hepatocytes in the liver were infected with HCV and, therefore, the possible reduction of GLUT2 mRNA expression in HCV-infected hepatocytes might have been masked by the normal levels of expression in uninfected hepatocytes concomitantly present in the same tissue samples.

It should also be noted that GLUT2 staining was also reduced in hepatocytes obtained from HBV-infected patients, though to a lesser extent than that from HCV-infected ones (Table 2). We assume that inflammatory responses in the liver may trigger some intracellular event that leads to decreased GLUT2 expression in hepatocytes *in vivo*.

In conclusion, we have demonstrated for the first time that HCV replication inhibits cellular glucose uptake through down-regulation of cell surface expression of GLUT2 and possibly GLUT1. It is conceivable that the decreased glucose uptake by hepatocytes causes impaired glucose metabolism, leading eventually to the initiation and progression of diabetes mellitus during a prolonged period of HCV persistence.

Acknowledgements

The authors are grateful to Dr. C.M. Rice (The Rockefeller University, New York, NY, USA) for providing pFL-J6/JFH1 and Huh7.5 cells. Thanks are also due to Dr. R. Bartenschlager (University of Heidelberg, Heidelberg, Germany) for providing an HCV subgenomic RNA replicon (pFK5B/2884Gly) and Dr. R. Sato (The University of Tokyo, Tokyo, Japan) for providing a human SREBP-1c expression plasmid (pME-hSREBP-1c). This study was supported in part by grants-in-aid for Scientific Research from the Ministry of Education, Culture, Sports, Science and Technology (MEXT) and the Ministry of Health, Labour and Welfare, Japan. This study was also carried out as part of the Program of Founding Research Centers for Emerging and Reemerging Infectious Diseases, MEXT, Japan, and the Global Center of Excellence (COE) Program at Kobe University Graduate School of Medicine.

Appendix A. Supplementary data

Supplementary data associated with this article can be found, in the online version, at doi:10.1016/j.jhep.2008.12.029.

References

[1] Simmonds P, Bukh J, Combet C, Deléage G, Enomoto N, Feinstone S, et al. Consensus proposals for a unified system of nomenclature of hepatitis C virus genotypes. Hepatology 2005;42:962–973.

[2] Lu L, Li C, Fu Y, Thaikruea L, Thongswat S, Maneekarn N, et al. Complete genomes for hepatitis C virus subtypes 6f, 6i, 6j and 6m: viral genetic diversity among Thai blood donors and infected spouses. J Gen Virol 2007;88:1505–1518.

[3] Lindenbach BD, Rice CM. Unravelling hepatitis C virus replication from genome to function. Nature 2005;436:933–938.

[4] Appel N, Schaller T, Penin F, Bartenschlager R. From structure to function: new insights into hepatitis C virus RNA replication. J Biol Chem 2006;281:9833–9836.

[5] Shepard CW, Finelli L, Alter MJ. Global epidemiology of hepatitis C virus infection. Lancet Infect Dis 2005;5:558–567.

[6] Galossi A, Guarisco R, Bellis L, Puoti C. Extrahepatic manifestations of chronic HCV infection. J Gastrointestin Liver Dis 2007;16:65–73.

[7] Caronia S, Taylor K, Pagliaro L, Carr C, Palazzo U, Petrik J, et al. Further evidence for an association between non-insulin-dependent diabetes mellitus and chronic hepatitis C virus infection. Hepatology 1999;30:1059–1063.

[8] Mason AL, Lau JY, Hoang N, Qian K, Alexander GJ, Xu L, et al. Association of diabetes mellitus and chronic hepatitis C virus infection. Hepatology 1999;29:328–333.

[9] Mehta S, Levey JM, Bonkovsky HL. Extrahepatic manifestations of infection with hepatitis C virus. Clin Liver Dis 2001;5:979–1008.

[10] Mehta SH, Brancati FL, Sulkowski MS, Strathdee SA, Szklo M, Thomas DL. Prevalence of type 2 diabetes mellitus among persons with hepatitis C virus infection in the United States. Ann Intern Med 2000;133:592–599.

[11] Wu X, Freeze HH. GLUT14, a duplicon of GLUT3, is specifically expressed in testis as alternative spice forms. Genomics 2002;80:553–557.

[12] Macheda ML, Rogers S, Best JD. Molecular and cellular regulation of glucose transporter (GLUT) proteins in cancer. J Cell Physiol 2005;202:654–662.

[13] Godoy A, Ulloa V, Rodriguez F, Reinicke K, Yanez AJ, Garcia Mde L, et al. Differential subcellular distribution of glucose transporters GLUT1-6 and GLUT9 in human cancer: ultrastructural localization of GLUT1 and GLUT5 in breast tumor tissues. J Cell Physiol 2006;207:614–627.

[14] Ban N, Yamada Y, Someya Y, Miyawaki K, Ihara Y, Hosokawa M, et al. Hepatocyte nuclear factor-1α recruits the transcriptional co-activator p300 on the GLUT2 gene promoter. Diabetes 2002;51:1409–1418.

[15] Blight KJ, McKeating JA, Rice CM. Highly permissive cell lines for subgenomic and genomic hepatitis C virus RNA replication. J Virol 2002;76:13001–13014.

[16] Hidajat R, Nagano-Fujii M, Deng L, Tanaka M, Takigawa Y, Kitazawa S, et al. Hepatitis C virus NS3 protein interacts with ELKS-δ and ELKS-α, members of a novel protein family involved in intracellular transport and secretory pathways. J Gen Virol 2005;86:2197–2208.

[17] Nomura-Takigawa Y, Nagano-Fujii M, Deng L, Kitazawa S, Ishido S, Sada K, et al. Non-structural protein 4A of Hepatitis C virus accumulates on mitochondria and renders the cells prone to undergoing mitochondria-mediated apoptosis. J Gen Virol 2006;87:1935–1945.

[18] Inubushi S, Nagano-Fujii M, Kitayama K, Tanaka M, An C, Yokozaki H, et al. Hepatitis C virus NS5A protein interacts with and negatively regulates the non-receptor protein–tyrosine kinase Syk. J Gen Virol 2008;89:1231–1242.

[19] Ikeda M, Abe K, Dansako H, Nakamura T, Naka K, Kato N. Efficient replication of a full-length hepatitis C virus genome, strain O, in cell culture, and development of a luciferase reporter system. Biochem Biophys Res Commun 2005;329:1350–1359.

[20] Deng L, Nagano-Fujii M, Tanaka M, Nomura-Takigawa Y, Ikeda M, Kato N, et al. NS3 protein of Hepatitis C virus associates with the tumour suppressor p53 and inhibits its

function in an NS3 sequence-dependent manner. J Gen Virol 2006;87:1703–1713.
[21] Lindenbach BD, Evans MJ, Syder AJ, Wolk B, Tellinghuisen TL, Liu CC, et al. Complete replication of hepatitis C virus in cell culture. Science 2005;309:623–626.
[22] Deng L, Adachi T, Kitayama K, Bungyoku Y, Kitazawa S, Ishido S, et al. Hepatitis C virus infection induces apoptosis through a Bax-triggered, mitochondrion-mediated, caspase 3-dependent pathway. J Virol 2008;82:10375–10385.
[23] Kanda H, Tamori Y, Shinoda H, Yoshikawa M, Sakaue M, Udagawa J, et al. Adipocytes from Munc18c-null mice show increased sensitivity to insulin-stimulated GLUT4 externalization. J Clin Invest 2005;115:291–301.
[24] Niwa H, Yamamura K, Miyazaki J. Efficient selection for high-expression transfectants with a novel eukaryotic vector. Gene 1991;108:193–199.
[25] Lehner PJ, Hoer S, Dodd R, Duncan LM. Downregulation of cell surface receptors by the K3 family of viral and cellular ubiquitin E3 ligase. Immunol Rev 2005;207:112–125.
[26] Mehta SH, Brancati FL, Strathdee SA, Pankow JS, Netski D, Coresh J, et al. Hepatitis C virus infection and incident type 2 diabetes. Hepatology 2003;38:50–56.
[27] Wang CS, Wang ST, Yao WJ, Chang TT, Chou P. Hepatitis C virus infection and the development of type 2 diabetes in a community-based longitudinal study. Am J Epidemiol 2007;166:196–203.
[28] Hui JM, Sud A, Farrell GC, Bandara P, Byth K, Kench JG, et al. Insulin resistance is associated with chronic hepatitis C virus infection and fibrosis progression. Gastroenterology 2003;125:1695–1704.
[29] Kawaguchi T, Yoshida T, Harada M, Hisamoto T, Nagao Y, Ide T, et al. Hepatitis C virus down-regulates insulin receptor substrates 1 and 2 through up-regulation of suppressor of cytokine signaling 3. Am J Pathol 2004;165:1499–1508.
[30] Miyamoto H, Moriishi K, Moriya K, Murata S, Tanaka K, Suzuki T, et al. Involvement of the PA28γ-dependent pathway in insulin resistance induced by hepatitis C virus core protein. J Virol 2007;81:1727–1735.
[31] Ader M, Ni TC, Bergman RN. Glucose effectiveness assessed under dynamic and steady state conditions. Comparability of uptake versus production components. J Clin Invest 1997;99:1187–1199.
[32] Banerjee S, Saito K, Ait-Goughoulte M, Meyer K, Ray RB, Ray R. Hepatitis C virus core protein upregulates serine phosphorylation of IRS-1 and impairs downstream Akt/PKB signaling pathway for insulin resistance. J Virol 2008;82:2606–2612.
[33] Im SS, Kim SY, Kim HI, Ahn YH. Transcriptional regulation of glucose sensors in pancreatic beta cells and liver. Curr Diabetes Rev 2006;2:11–18.
[34] Adachi T, Yasuda K, Okamoto Y, Shihara N, Oku A, Ueta K, et al. T-1095, a renal Na^+-glucose transporter inhibitor, improves hyperglycemia in streptozotocin-induced diabetic rats. Metabolism 2000;49:990–995.
[35] Im SS, Kang SY, Kim SY, Kim HI, Kim JW, Kim KS, et al. Glucose-stimulated upregulation of GLUT2 gene is mediated by sterol response element-binding protein-1c in the hepatocytes. Diabetes 2005;54:1684–1691.
[36] Kanayama T, Arito M, So K, Hachimura S, Inoue J, Sato R. Interaction between sterol regulatory element-binding proteins and liver receptor homolog-1 reciprocally suppresses their transcriptional activities. J Biol Chem 2007;282:10290–10298.

JOURNAL OF VIROLOGY, Mar. 2009, p. 2338–2348 Vol. 83, No. 5
0022-538X/09/$08.00+0 doi:10.1128/JVI.01840-08

Arsenic Trioxide Inhibits Hepatitis C Virus RNA Replication through Modulation of the Glutathione Redox System and Oxidative Stress[▽]

Misao Kuroki,[1] Yasuo Ariumi,[1] Masanori Ikeda,[1] Hiromichi Dansako,[1] Takaji Wakita,[2] and Nobuyuki Kato[1]*

Department of Tumor Virology, Okayama University Graduate School of Medicine, Dentistry, and Pharmaceutical Sciences, 2-5-1, Shikata-cho, Okayama 700-8558, Japan,[1] and Department of Virology II, National Institute of Infectious Diseases, 1-23-1 Toyama, Shinjuku-ku, Tokyo 162-8640, Japan[2]

Received 2 September 2008/Accepted 13 December 2008

Arsenic trioxide (ATO), a therapeutic reagent used for the treatment of acute promyelocytic leukemia, has recently been reported to increase human immunodeficiency virus type 1 infectivity. However, in this study, we have demonstrated that replication of genome-length hepatitis C virus (HCV) RNA (O strain of genotype 1b) was notably inhibited by ATO at submicromolar concentrations without cell toxicity. RNA replication of HCV-JFH1 (genotype 2a) and the release of core protein into the culture supernatants were also inhibited by ATO after the HCV infection. To clarify the mechanism of the anti-HCV activity of ATO, we examined whether or not PML is associated with this anti-HCV activity, since PML is known to be a target of ATO. Interestingly, we observed the cytoplasmic translocation of PML after treatment with ATO. However, ATO still inhibited the HCV RNA replication even in the PML knockdown cells, suggesting that PML is dispensable for the anti-HCV activity of ATO. In contrast, we found that *N*-acetyl-cysteine, an antioxidant and glutathione precursor, completely and partially eliminated the anti-HCV activity of ATO after 24 h and 72 h of treatment, respectively. In this context, it is worth noting that we found an elevation of intracellular superoxide anion radical, but not hydrogen peroxide, and the depletion of intracellular glutathione in the ATO-treated cells. Taken together, these findings suggest that ATO inhibits the HCV RNA replication through modulation of the glutathione redox system and oxidative stress.

Hepatitis C virus (HCV) is the causative agent of chronic hepatitis, which progresses to liver cirrhosis and hepatocellular carcinoma. HCV is an enveloped virus with a positive single-stranded 9.6-kb RNA genome, which encodes a large polyprotein precursor of approximately 3,000 amino acid residues. This polyprotein is cleaved by a combination of the host and viral proteases into at least 10 proteins in the following order: core, envelope 1 (E1), E2, p7, nonstructural 2 (NS2), NS3, NS4A, NS4B, NS5A, and NS5B (30).

Alpha interferon has been used as an effective anti-HCV reagent in clinical therapy for patients with chronic hepatitis C. The current combination treatment with pegylated alpha interferon and ribavirin, a nucleoside analogue, has been shown to improve the sustained virological response rate to more than 50% (15). However, the adverse effects of the combination therapy and the limited efficacy against genotype 1b warrant the development of new anti-HCV reagents.

Arsenic trioxide (ATO) (As_2O_3, arsenite) has been used as a therapeutic reagent in acute promyelocytic leukemia, which bears an oncogenic PML-retinoic acid receptor alpha fusion protein resulting from chromosomal translocation (51, 52, 68, 70). The ATO treatment induces complete remission through degradation of the aberrant PML-retinoic acid receptor α (70). The PML tumor suppressor protein is required for formation of the PML nuclear body (PML-NB), also known as nuclear dot 10 or the PML oncogenic domain, which is often disrupted by infection with DNA viruses, such as herpes simplex virus type 1, human cytomegalovirus, and Epstein-Barr virus (17). The treatment with ATO results in degradation of the PML protein and disruption of the PML-NB (70). Therefore, ATO has been become a useful probe for investigating the functions of the PML-NB, including cell growth, apoptosis, stress response, and viral infection. Indeed, ATO has been shown to increase retroviral infectivity, such as human immunodeficiency virus type 1 (HIV-1) and murine leukemia virus infectivity, but the mechanisms of this change are not well understood (5, 6, 32, 44, 47, 50, 57). In contrast, ATO was recently reported to inhibit the replication of HCV subgenomic replicon RNA (24). However, it also remains unclear how ATO inhibits the HCV RNA replication. In this study, using genome-length HCV RNA replication systems, we investigated the molecular mechanism(s) of the anti-HCV activity of ATO, and we provide evidence that ATO inhibits HCV RNA replication through modulation of the glutathione redox system and oxidative stress.

MATERIALS AND METHODS

Reagents. ATO, *N*-acetyl-cysteine (NAC), ascorbic acid (vitamin C), and L-buthionine sulfoximine (BSO) were purchased from Sigma (St. Louis, MO). Arsenic pentoxide (APO) (As_2O_5, arsenate) was purchased from Wako (Osaka, Japan). Both ATO and APO were dissolved in 1 N NaOH at 0.1 M as a stock solution. An inducible nitric oxide synthase (iNOS) inhibitor, 1400W, was purchased from Calbiochem (Merck Biosciences, Darmstadt, Germany).

Cell culture. 293FT cells were cultured in Dulbecco's modified Eagle's medium (Invitrogen, Carlsbad, CA, USA) supplemented with 10% fetal bovine serum. The following four HuH-7-derived cell lines or their parental HuH-7 cells

* Corresponding author. Mailing address: Department of Tumor Virology, Okayama University Graduate School of Medicine, Dentistry, and Pharmaceutical Sciences, 2-5-1, Shikata-cho, Okayama 700-8558, Japan. Phone: 81 86 235 7385. Fax: 81 86 235 7392. E-mail: nkato@md.okayama-u.ac.jp.

▽ Published ahead of print on 24 December 2008.

were cultured in Dulbecco's modified Eagle's medium with 10% fetal bovine serum as described previously (25): O cells, harboring a replicative genome-length HCV-O RNA (O strain of genotype 1b) (25); OR6 cells, harboring the genome-length HCV-O RNA with luciferase as a reporter (25); sO cells, harboring the subgenomic replicon RNA of HCV-O (31); and RSc cured cells, which cell culture-generated HCV-JFH1 (JFH1 strain of genotype 2a) (58) could infect and effectively replicate in (2, 3). The O, OR6, and sO cells were maintained in the presence of G418 (300 μg/ml Geneticin; Invitrogen).

RNA interference. Oligonucleotides with the following sense and antisense sequences were used for the cloning of short hairpin RNA (shRNA)-encoding sequences targeted to PML (56) in a lentiviral vector: 5′-GATCCCCAGATGC AGCTGTATCCAAGTTCAAGAGACTTGGATACAGCTGCATCTTTTTTG GAAA-3′ (sense) and 5′-AGCTTTTCCAAAAAAGATGCAGCTGTATCCAA GTCTCTTGAACTTGGATACAGCTGCATCTGGG-3′ (antisense). These oligonucleotides were annealed and subcloned into the BglII-HindIII site, downstream from an RNA polymerase III promoter of pSUPER (8), to generate pSUPER-PMLi. To construct pLV-PMLi, the BamHI-SalI fragments of pSUPER-PMLi were subcloned into the BamHI-SalI site of pRDI292, an HIV-1-derived self-inactivating lentiviral vector containing a puromycin resistance marker allowing for the selection of transduced cells (7). pLV-Chk2i was described previously (3).

Lentiviral vector production. The vesicular stomatitis virus (VSV) G-pseudotyped HIV-1-based vector system has been described previously (42). The lentiviral vector particles were produced by transient transfection of the second-generation packaging construct pCMV-ΔR8.91 (1, 71) and the VSV G envelope-expressing plasmid pMDG2 as well as pRDI292 into 293FT cells with FuGene6 (Roche Diagnostics, Mannheim, Germany).

HCV infection experiments. The supernatants was collected from cell culture-generated HCV-JFH1 (58)-infected RSc cells (2, 3) at 5 days postinfection and stored at −80°C after filtering through a 0.45-μm filter (Kurabo, Osaka, Japan) until use. For infection experiments with HCV-JFH1 virus, RSc cells (1×10^5 cells/well) were plated onto six-well plates and cultured for 24 h. We then infected the cells with 50 μl (equivalent to a multiplicity of infection of 0.05 to 0.1) of inoculum. The culture supernatants were collected at 97 h postinfection, and the levels of the core protein were determined by enzyme-linked immunosorbent assay (Mitsubishi Kagaku Bio-Clinical Laboratories, Tokyo, Japan). Total RNA was isolated from the infected cellular lysates using an RNeasy minikit (Qiagen, Hilden, Germany) for quantitative reverse transcription-PCR (RT-PCR) analysis of intracellular HCV RNA. The level of intracellular HCV RNA in the RSc cells was $>10^8$ copies/μg total RNA at 4 days postinfection.

Quantitative RT-PCR Analysis. The quantitative RT-PCR analysis for HCV RNA was performed by real-time LightCycler PCR (Roche) as described previously (25). We used the following forward and reverse primer sets for the real-time LightCycler PCR: PML, 5′-GAGGAGTTCCAGTTTCTGCG-3′ (forward), 5′-GCGCCTGGCAGATGGGGCAC-3′ (reverse); β-actin, 5′-TGACGG GGTCACCCACACTG-3′ (forward), 5′-AAGCTGTAGCCGCGCTCGGT-3′ (reverse); HCV-O, 5′-AGAGCCATAGTGGTCTGCGG-3′ (forward), 5′-CTT TCGCGACCCAACACTAC-3′ (reverse); and HCV-JFH1, 5′-5′-AGAGCCAT AGTGGTCTGCGG-3′ (forward), 5′-CTTTCGCAACCCAACGCTAC-3′ (reverse).

Western blot analysis. Cells were lysed in buffer containing 50 mM Tris-HCl (pH 8.0), 150 mM NaCl, 4 mM EDTA, 1% Nonidet P-40, 0.1% sodium dodecyl sulfate, 1 mM dithiothreitol, and 1 mM phenylmethylsulfonyl fluoride. Supernatants from these lysates were subjected to sodium dodecyl sulfate-polyacrylamide gel electrophoresis, followed by immunoblot analysis using anti-PML (A301-168A-1; Bethyl Laboratories, Montgomery, TX), anti-Chk2 (DCS-273; Medical & Biological Laboratories, MBL, Nagoya, Japan), anti-HCV core (CP-9 and CP-11; Institute of Immunology, Tokyo, Japan), anti-HCV NS5A (no. 8926; a generous gift from A Takamizawa, The Research Foundation for Microbial Diseases of Osaka University, Japan), anti-signal transducer and activator of transcription 3 (anti-STAT3) (BD Bioscience, San Jose, CA), anti-phospho-STAT3 (Tyr705) (Cell Signaling Technology, Danvers, MA) anti-poly(ADP-ribose) polymerase 1 (anti-PARP-1) (C-2-10; Calbiochem), or anti-β-actin antibody (Sigma).

MTT assay. HuH-7 or O cells (5×10^3 cells/well) were plated onto 96-well plates and cultured for 24 h. The cells were treated with ATO, APO, or NaOH for 24, 48, or 72 h and then subjected to the colorimetric 3-(4,5-dimethylthiazol-2-yl)-2,5-diphenyltetrazolium bromide (MTT) assay according to the manufacturer's instructions (cell proliferation kit I; Roche). The absorbance was read using a microplate reader (model 2550; Bio-Rad Laboratories, Hercules, CA) at 550 nm with a reference wavelength of 690 nm.

RL assay. OR6 cells (1.5×10^4 cells/well) were plated onto 24-well plates and cultured for 24 h. The cells were treated with each reagent for 72 h and then subjected to the *Renilla* luciferase (RL) assay according to the manufacturer's instructions (Promega, Madison, WI). A Lumat LB9507 luminometer (Berthold, Bad Wildbad, Germany) was used to detect RL activity.

FL assay. Plasmids were transfected into O cells (2×10^4 cells/well in 24-well plates) using FuGene6 and cultured for 24 h. The cells were treated with or without 1 μM ATO for 24 h, and then firefly luciferase (FL) assays were performed according to the manufacturer's instructions (Promega).

Immunofluorescence and confocal microscopic analysis. Cells were fixed in 3.6% formaldehyde in phosphate-buffered saline (PBS), permeabilized in 0.1% NP-40 in PBS at room temperature, and incubated with anti-PML antibody (PM001; MBL) at a 1:300 dilution in PBS containing 3% bovine serum albumin at 37°C for 30 min. They were then stained with fluorescein isothiocyanate-conjugated anti-rabbit antibody (Jackson ImmunoResearch, West Grove, PA) at a 1:300 dilution in PBS containing bovine serum albumin at 37°C for 30 min, followed by staining with 4′,6-diamidino-2-phenylindole (DAPI) at room temperature for 15 min. Following extensive washing in PBS, the cells were mounted on slides using a mounting medium of 90% glycerin–10% PBS with 0.01% *p*-phenylenediamine added to reduce fading. Samples were viewed under a confocal laser-scanning microscope (LSM510; Zeiss, Jena, Germany).

Measurement of intracellular O_2^- and H_2O_2 production. The intracellular superoxide anion radical (O_2^-) levels were measured with an oxidation-sensitive fluorescent probe, dihydroethidium (DHE) (Invitrogen Molecular Probes), that is highly selective for detection of O_2^- among reactive oxygen species (ROS). DHE is cell permeative and reacts with O_2^- to form ethidium, which in turn intercalates in DNA, thereby exhibiting a red fluorescence. The intracellular hydrogen peroxide (H_2O_2) levels were measured with another oxidation-sensitive fluorescent probe dye, 6-carboxy-2′,7′-dichlorodihydrofluorescein diacetate (carboxy-H_2DCFDA) (Invitrogen Molecular Probes). Carboxy-H_2DCFDA was intracellularly deacetylated with esterase and further oxidized with peroxidase to the fluorescent 2′,7′-dichlorodihydrofluorescein (DCF). The ATO- or BSO-treated O cells were washed with PBS and incubated with 5 μM DHE and 20 μM carboxy-H_2DCFDA in PBS at 37°C for 30 min. Cells were then washed twice with PBS. The DHE or DCF fluorescence intensity was measured using a FACSCalibur flow cytometer. For each sample, 10,000 events were collected. The O_2^- or H_2O_2 levels are indicated as mean fluorescence intensities, which were determined with the CellQuest software (BD Bioscience).

Detection of intracellular glutathione. Intracellular glutathione levels were analyzed using CellTracker Green (5-chloromethylfluorescein diacetate [CMFDA]; Molecular Probes, Invitrogen). CMFDA is a membrane-permeative dye used to determine intracellular glutathione levels. Cytoplasmic esterase converts the nonfluorescent CMFDA to the fluorescent 5-chloromethylfluorescein (CMF), which can then react with glutathione. The excitation peak is at 492 nm, and the fluorescence emission peak is at 517 nm. O cells treated with 1 μM ATO for 72 h were washed with PBS and incubated with 5 μM CMFDA at 37°C for 30 min. The CMF fluorescence intensity was measured using a FACSCalibur flow cytometer. For each sample, 10,000 events were collected. The glutathione levels are given as the relative mean fluorescence intensities, which were determined with CellQuest software.

RESULTS

ATO inhibits HCV RNA replication. First, we quantitatively examined the effect of ATO on the HCV RNA replication in HuH-7-derived O cells harboring a replicative genome-length HCV-O RNA (25). We found that submicromolar concentrations of ATO markedly inhibited genome-length HCV-O RNA replication in the O cells at 72 h after administration (Fig. 1A). The 50% effective concentration (EC_{50}) of ATO required for inhibition of genome-length HCV-O RNA replication was 0.19 μM (Fig. 1A). Consistent with this finding, the expression levels of the HCV core and NS5A proteins were also significantly decreased in the cell lysates of O cells treated with ATO for 72 h (Fig. 1B). In addition, ATO markedly inhibited the replication of the subgenomic replicon RNA (31), with an EC_{50} of 0.48 μM at 72 h after the treatment (Fig. 1C). We next examined the effect of ATO on HCV reproduction by HCV-JFH1 infection (58). The results revealed that ATO significantly inhibited the intracellular RNA replication of HCV-

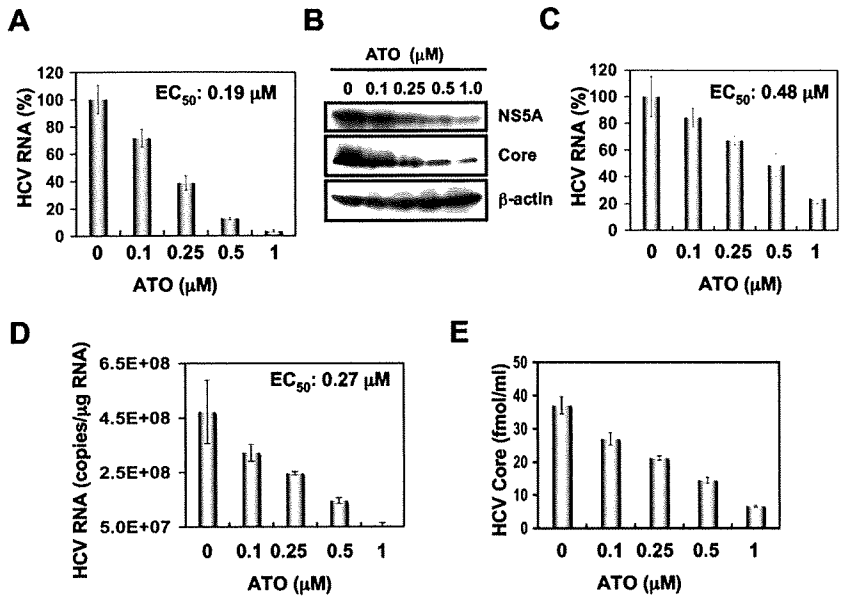

FIG. 1. Inhibition of HCV RNA replication by ATO. (A) The level of genome-length HCV RNA in O cells after the treatment with ATO was monitored by real-time LightCycler PCR. Experiments were done in triplicate and, bars represent the mean percentage of HCV RNA. Error bars indicate standard deviations. (B) HCV core and NS5A protein expression levels in O cells after treatment with ATO. The results of Western blot analysis of cellular lysates with anti-HCV core, anti-HCV NS5A, or anti-β-actin antibody in O cells at 72 h after treatment with ATO at the indicated concentration are shown. (C) The level of subgenomic replicon RNA was monitored by real-time LightCycler PCR. Results from three independent experiments conducted as described for panel A are shown. (D) The level of intracellular genome-length HCV-JFH1 RNA was monitored by real-time LightCycler PCR. RSc cells were pretreated with the indicated concentration of ATO for 13 h, followed by inoculation of the HCV-JFH1 virus, and then the infected cells were further incubated with ATO for 97 h. Results from three independent experiments conducted as described for panel A are shown. (E) The levels of the core protein in the culture supernatants treated as described for panel D were determined by enzyme-linked immunosorbent assay. Experiments were done in triplicate, and bars represent the mean core protein levels.

JFH1, with an EC_{50} of 0.27 μM, as well as the release of core protein into the culture supernatants in HuH-7-derived RSc cells at 97 h after inoculation of the HCV-JFH1 virus (Fig. 1D and E). Thus, we have demonstrated for the first time that ATO can inhibit the reproduction of HCV and particularly HCV RNA replication.

Effect of APO on HCV replication. Arsenic is known to exist in two oxidation states, As(III) in ATO and As(V) in APO. As ATO in the lower valence state has been reported to be more toxic than APO (48), we compared their anti-HCV activities using an OR6 assay system, which was recently developed as a luciferase reporter assay system for monitoring genome-length HCV RNA replication in HuH-7-derived OR6 cells (Fig. 2A) (25). The results showed that APO could not strongly suppress HCV replication at submicromolar concentrations, while ATO strongly inhibited it, with an EC_{50} of 0.33 μM (Fig. 2B and C), indicating that ATO has unique anti-HCV activity. In this context, it is relevant that the expression level of HCV core protein was also remarkably decreased in the cell lysates of O cells treated with ATO, but not those treated with APO, for 72 h (Fig. 2D). Thus, APO seems to be a useful negative probe to clarify the mechanism of the anti-HCV activity of ATO.

ATO does not affect cell growth at submicromolar concentrations. ATO has been reported to induce apoptosis (11, 14, 20, 21, 26–28, 33, 48, 66). Therefore, such an ATO-induced apoptosis may be involved in the anti-HCV activity. To test this possibility, we examined the effect of ATO or APO at various concentrations on cell proliferation by colorimetric MTT assay. In this context, we demonstrated that ATO did not affect the cell proliferation of O cells or the parental HCV-negative HuH-7 cells at submicromolar concentrations (Fig. 3A and E). In contrast, 4 or 8 μM ATO significantly inhibited cell proliferation (Fig. 3B and F). Similarly, APO did not affect the cell proliferation at less than 2 μM (Fig. 3C and D). Consistent with the above results, ATO-treated O cells exhibited normal growth rates and cell viabilities, at least at 1 μM for 72 h (Fig. 3G). Furthermore, we did not observe the cleavage of PARP-1, which is known to be an important substrate for activated caspase 3, in O cells treated with 1 μM ATO at least until 72 h (Fig. 3H), indicating that 1 μM ATO did not induce apoptosis in O cells. Thus, we concluded that the anti-HCV activity was independent of ATO-induced apoptosis or cell toxicity, at least at submicromolar concentrations.

PML and Chk2 are dispensable for the anti-HCV activity of ATO. Since PML is known to be a target of ATO (70), we first examined the subcellular localization of PML in O cells treated with either 1 μM ATO or 1 μM APO for 72 h by means of an anti-PML antibody (PM001; MBL) that can recognize most of the PML splicing variants and is useful for immunofluorescence analysis. The results showed that PML was localized predominantly in punctate nuclear speckles termed PML-NBs in control O cells (Fig. 4A). Interestingly, we noticed that some nuclear PML, but not all, disappeared and was translocated into discrete cytoplasmic bodies in the O cells treated with 1 μM ATO (Fig. 4A). We also observed cytoplasmic translocation of PML in the O cells treated with 1 μM APO for 72 h (Fig. 4A). Furthermore, we observed a similar cytoplasmic translocation of PML in the HCV-negative 293FT or HeLa

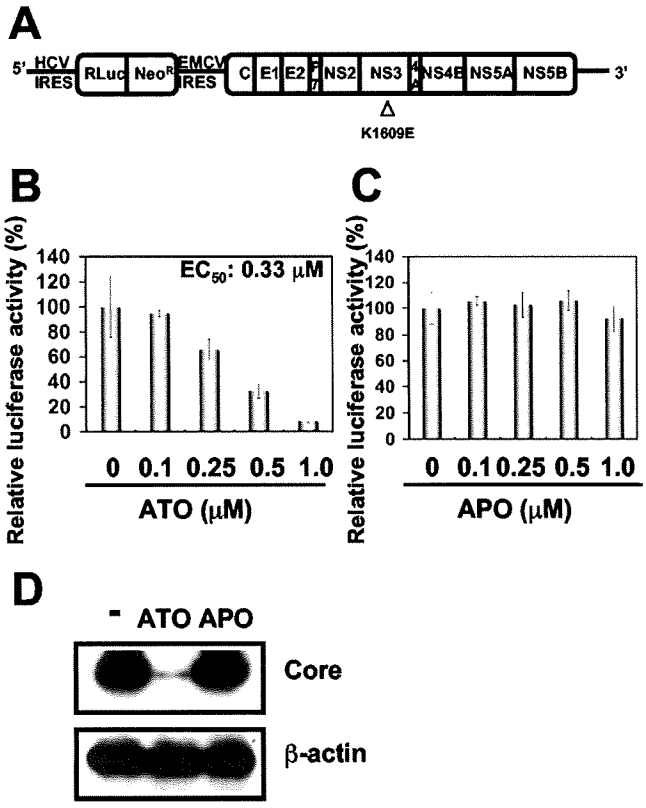

FIG. 2. Effect of APO on HCV replication. (A) Schematic representation of genome-length HCV RNA encoding the RL gene as a reporter (ORN/C-5B/KE RNA) replicated in OR6 cells. The RL is expressed as a fusion protein with neomycin phosphotransferase (Neo^R). The position of an adaptive mutation, K1609E in NS3, is indicated by an open triangle. (B) Effect of ATO on genome-length HCV RNA replication. At 72 h after treatment of OR6 cells with ATO at the indicated concentrations, the replication level of HCV RNA was monitored by the RL assay. The relative RL activity is shown. The results shown are means from three independent experiments. Error bars indicate standard deviations. (C) Effect of APO on genome-length HCV RNA replication. At 72 h after treatment of OR6 cells with APO at the indicated concentrations, the replication level of HCV RNA was monitored by the RL assay as described for panel B. (D) HCV core protein expression level in O cells after treatment with either ATO or APO. The results of Western blot analysis of cellular lysates with anti-HCV core or anti-β-actin antibody in O cells at 72 h after treatment with either 1 μM ATO or 1 μM APO are shown.

cells after the treatment with ATO (data not shown). Thus, we concluded that the cytoplasmic translocation of PML after the treatment with ATO was not associated with anti-HCV activity. Next, Western blot analysis to compare PML expression in the lysates of O cells treated with 1 μM ATO or 1 μM APO for 72 h was performed using another anti-PML antibody, A301-168A-1 (a gift from Bethyl Laboratories), which can recognize the longest isoform, PML I, but not shorter PML isoforms such as PML VI and which has been proven useful for Western blot analysis. Consistent with the previous finding that ATO promotes PML degradation (70), the expression level of the PML I protein was lower in the ATO-treated O cells than in the APO-treated O cells (Fig. 4B), suggesting that PML degradation by ATO is associated with anti-HCV activity. To further examine whether PML is directly involved in the anti-HCV activity of ATO, we used lentiviral vector-mediated RNA interference to stably knock down PML in the O cells. To express an shRNA targeted to all PML isoforms (56), we used the VSV G-pseudotyped HIV-1-based vector system (1, 42, 71). We used the puromycin-resistant pooled cells at 10 days after the lentiviral transduction in this experiment. Immunofluorescence and Western blot analysis demonstrated a very effective knockdown of PML in the O cells (Fig. 4C and D). We quantitatively examined the level of HCV RNA in the PML knockdown O cells treated with or without either 1 μM ATO (Fig. 4E) or 1 μM APO (Fig. 4F) for 72 h. The results showed that the replication level of genome-length HCV-O RNA in the untreated PML knockdown cells was similar to that in control cells (Fig. 4E), suggesting that PML is dispensable in HCV RNA replication. Importantly, ATO effectively inhibited the HCV RNA replication in both the PML knockdown cells and control cells compared with that of the APO-treated cells (Fig. 4E and F). Thus, we concluded that PML was dispensable for the anti-HCV activity of ATO. Since the Chk2 checkpoint kinase has recently been implicated in ATO-induced apoptosis and in association with PML (27, 63, 64, 66), we examined the anti-HCV activity in the ATO-treated Chk2 knockdown O cells (3). As we previously described, Western blot analysis demonstrated very effective knockdown of Chk2 in O cells (Fig. 4G). Accordingly, we examined the level of HCV RNA in Chk2 knockdown cells treated with or without either 1 μM ATO (Fig. 4H) or 1 μM APO (Fig. 4I) for 72 h. Consistent with our recent finding that Chk2 is required for HCV RNA replication, the replication of genome-length HCV RNA in the untreated Chk2 knockdown cells was remarkably suppressed (Fig. 4H). However, ATO strongly inhibited the HCV RNA replication in the Chk2 knockdown cells compared with that in the APO-treated Chk2 knockdown cells (Fig. 4H and I), suggesting that Chk2 is not implicated in the anti-HCV activity of ATO.

Effect of ATO on the stress-signaling pathways. To date, the focus has been on PML and PML-retinoic acid receptor α as major targets of ATO (70). On the other hand, arsenic has been reported to modulate other cell-signaling pathways, especially stress-responsive transcription factors, such as nuclear factor κB (NF-κB), activator protein 1 (AP-1), and STAT3 (12, 37, 38, 62). Therefore, we examined the involvement of several stress-responsive pathways in the anti-HCV activity of ATO by luciferase-based reporter assays or Western blot analysis using an antibody which specifically recognizes STAT3 phosphorylated at tyrosine 705. Although it has been reported that ATO inhibited the NF-κB signaling pathway through a direct interaction with IKKβ at a high concentration (more than 10 μM) (29), neither 1 μM ATO nor 1 μM APO affected the endogenous NF-κB transcriptional activity in the present study (Fig. 5A and B). Conversely, ATO at least slightly stimulated mitogen-activated protein kinase kinase kinase (MEKK)-mediated NF-κB activation (Fig. 5A and B). Since NF-κB activation has been shown to stimulate HCV replication (60), the NF-κB pathway would seem not to be essential for the anti-HCV activity of ATO. Next, regarding the AP-1 signaling pathway, both ATO and APO are known to activate c-Jun N-terminal kinase (JNK) (45). Importantly, there was no stimulation of JNK activity at a dose below 30 μM (45). In fact, 50 μM ATO but not 50 μM APO strongly stimulates AP-1 activity by in-

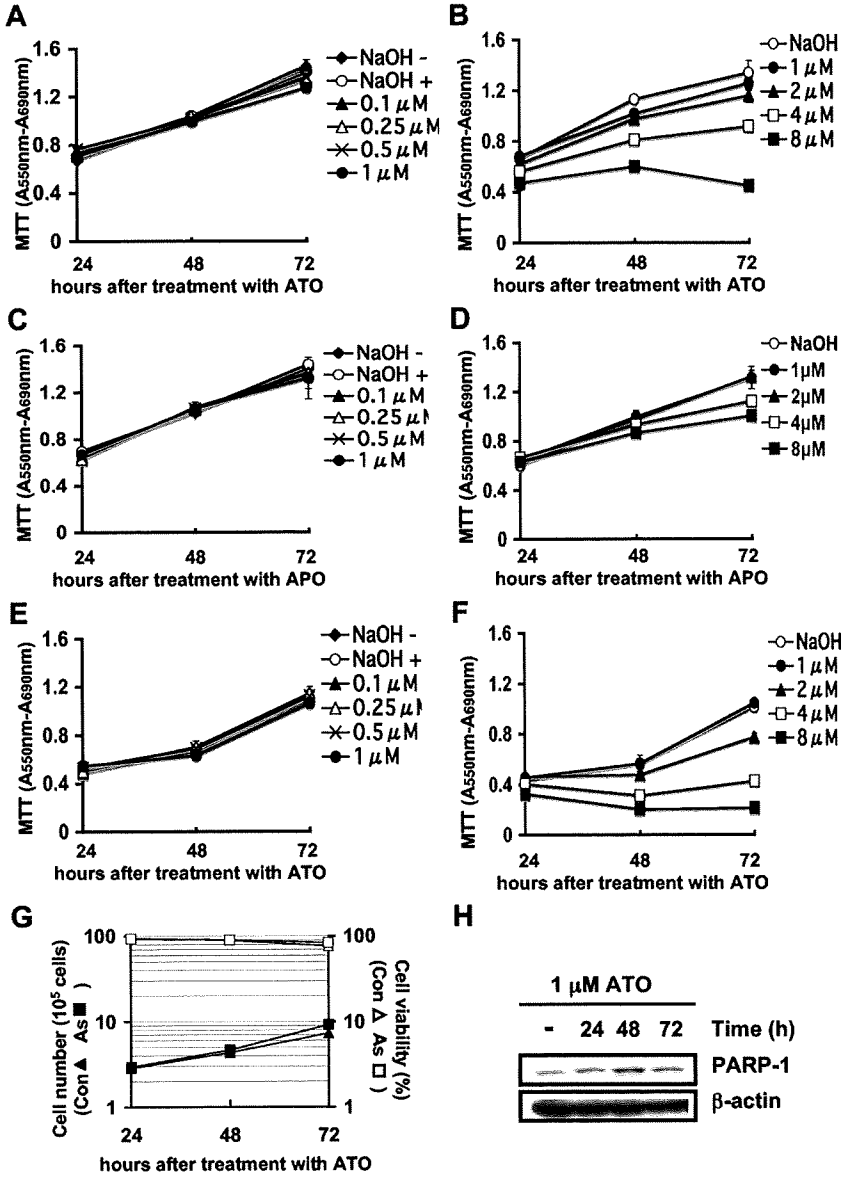

FIG. 3. Effect of ATO on cell growth and viability. (A and B) MTT assay of O cell lysates at the indicated times after treatment with ATO at various concentrations. NaOH (10 μM) was used as the solvent for ATO. The results shown are means from three independent experiments. Error bars indicate standard deviations. (C and D) MTT assay of O cell lysates at the indicated times after treatment with APO at various concentrations. (E and F) MTT assay of HuH-7 cell lysates at the indicated times after treatment with ATO at various concentrations. (G) Growth curve and viability of O cells after treatment with either 10 μM NaOH (Con) or 1 μM ATO (As). (H) Western blot analysis of cellular lysates with anti-PARP-1 or anti-β-actin antibody in O cells at the indicated times after treatment with 1 μM ATO.

hibiting a JNK phosphatase (10). Consistently, we found that both 1 μM ATO and 1 μM APO had a marginal effect on the AP-1 signaling pathway (Fig. 5C and D), suggesting that the AP-1 pathway is also not involved in the anti-HCV activity of ATO. Regarding the STAT3 signaling pathway, ATO has been reported to inhibit the phosphorylation of the STAT3 tyrosine at 705, leading to inactivation of the JAK-STAT signaling pathway (12, 62). In contrast, it has been reported that HCV constitutively phosphorylates and activates STAT3 (49, 59, 67). In this context, we observed constitutive tyrosine phosphorylation of STAT3 in untreated O cells (Fig. 5E). Furthermore, the marginal effect of 1 μM ATO on STAT3 phosphorylation and interleukin-6-mediated STAT3 activation was also observed (Fig. 5E and F). Taken together, these results at least suggest that the NF-κB, AP-1, and STAT3 pathways may not be associated with the anti-HCV activity of ATO at submicromolar concentrations.

The anti-HCV activity of ATO is associated with the glutathione redox system and oxidative stress. Finally, we focused on the involvement of the glutathione redox system and oxidative stress in the anti-HCV activity of ATO. For this, we analyzed the HCV replication level after combination treatment with ATO and antioxidants such as NAC and vitamin C using the OR6 assay system. When OR6 cells were treated with

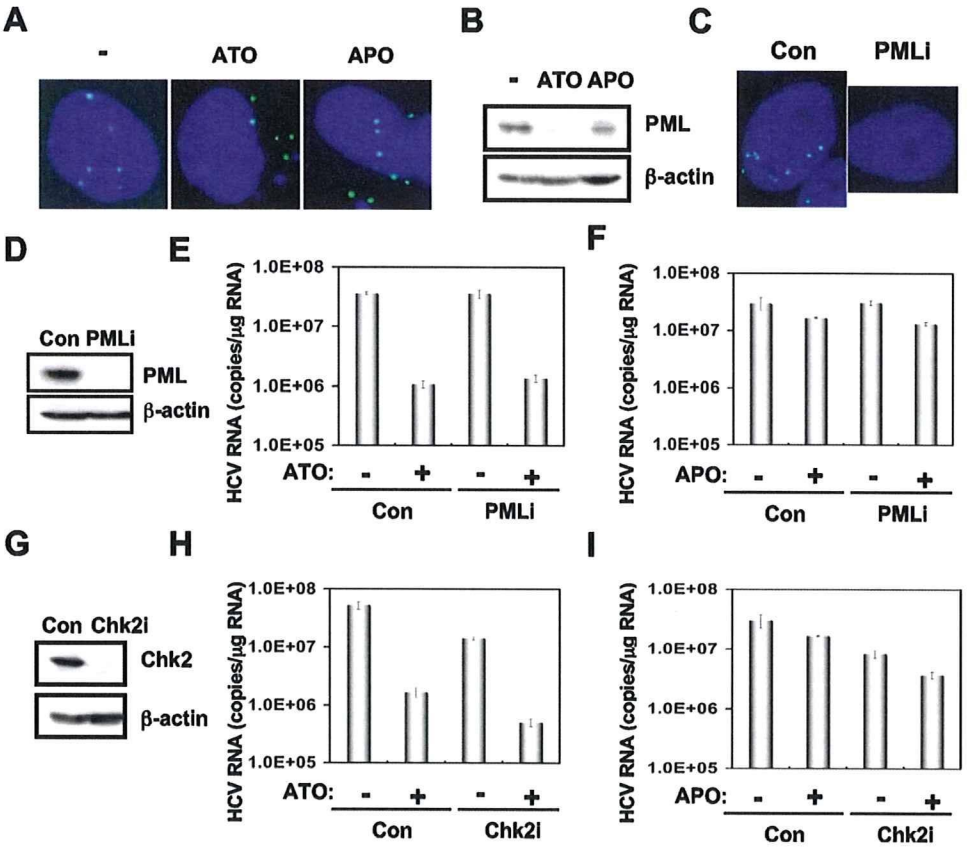

FIG. 4. PML and Chk2 are not required for the anti-HCV activity of ATO. (A) Subcellular localization of PML in O cells at 72 h after treatment with 10 μM NaOH (−), 1 μM ATO, or 1 μM APO. PML was detected by indirect immunofluorescence analysis with anti-PML antibody (PM001). DAPI staining of the nuclear DNA is also shown. (B) Induction of PML degradation by ATO but not by APO. The results of Western blot analysis of cellular lysates of O cells at 72 h after treatment with 10 μM NaOH (−), 1 μM ATO, or 1 μM APO with anti-PML (A301-168A-1) or anti-β-actin antibody are shown. (C) Stable knockdown of PML by shRNA-producing lentiviral vector in O cells. PML was detected by indirect immunofluorescence analysis with anti-PML antibody (PM001) in O cells expressing shRNA targeted to PML (PMLi) as well as in O cells transduced with a control lentiviral vector (Con). (D) Western blot analysis of cellular lysates with anti-PML (A301-168A-1) or anti-β-actin antibody in PML knockdown O cells (PMLi) as well as in control O cells (Con). (E and F) The level of genome-length HCV-O RNA was monitored by real-time LightCycler PCR in PML knockdown O cells (PMLi) as well as in control O cells (Con) after treatment with 10 μM NaOH (−), 1 μM ATO (+) (E), or 1 μM APO (+) (F) for 72 h. Results from three independent experiments conducted as described in the legend to Fig. 1A are shown. (G) Inhibition of Chk2 expression by shRNA-producing lentiviral vector. The results of Western blot analysis of cellular lysates with anti-Chk2 or anti-β-actin antibody in O cells expressing shRNA targeted to Chk2 (Chk2i) as well as in O cells transduced with a control lentiviral vector (Con) are shown. (H and I) The level of genome-length HCV-O RNA was monitored by real-time LightCycler PCR in Chk2 knockdown O cells (Chk2i) as well as in control O cells (Con) after treatment with 10 μM NaOH (−), 1 μM ATO (+) (H), or 1 μM APO (+) (I) for 72 h. Results from three independent experiments conducted as described in the legend to Fig. 1A are shown.

either 100 μM vitamin C or 10 mM NAC alone for 24 h or 72 h, the HCV replication was slightly enhanced (Fig. 6A and B), indicating that the antioxidant can activate HCV replication. Although the anti-HCV activity in the OR6 cells treated with 1 μM ATO and in combination with 100 μM vitamin C for 24 h was weakly reduced, 10 mM NAC completely and partially eliminated the anti-HCV activity of ATO after 24 h (Fig. 6A) and 72 h (Fig. 6B) of treatment, respectively, suggesting that oxidative stress and the glutathione redox system are associated with the anti-HCV activity of ATO. In contrast, the iNOS inhibitor 1400W did not suppress the HCV RNA replication or eliminate the anti-HCV activity of ATO, suggesting that NO is not involved in the anti-HCV activity of ATO (Fig. 6C). To further examine the involvement of oxidative stress in the anti-HCV activity of ATO, we examined ROS production in ATO-treated cells using two oxidative-sensitive fluorescent probes, DHE for detection of intracellular O_2^- and DCF for detection of intracellular H_2O_2. We found that 1 μM ATO could generate a significant level of intracellular O_2^- but not intracellular H_2O_2, while 2 μM BSO, an inhibitor of glutathione synthesis (14, 20, 33), could induce both O_2^- and H_2O_2 (Fig. 6D to H). Importantly, NAC diminished the ATO-dependent O_2^- induction (Fig. 6F). Since glutathione is a major antioxidant in cells and can clear away superoxide anion free radical, we also analyzed the changes of the intracellular glutathione level in ATO-treated O cells using CMF fluorescence, which can react with glutathione. As a result, we observed significant glutathione depletion in the cells treated with at least 1 μM ATO (Fig. 6I). To further confirm the involvement of glutathione in the anti-HCV activity of ATO, we examined the effect of cotreatment with ATO and BSO. When the OR6 cells were treated with 1 μM BSO alone, the HCV replication

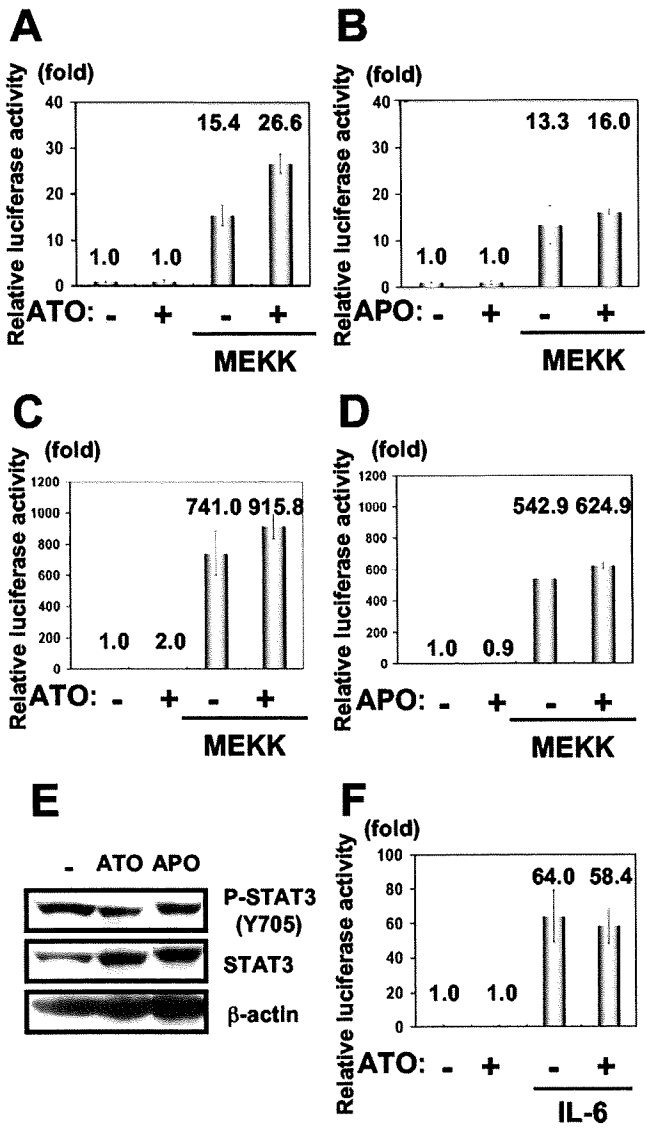

FIG. 5. Effect of ATO on the stress-signaling pathways. (A and B) Effect of ATO or APO on the NF-κB signaling pathway. O cells were transfected with 100 ng of reporter plasmid, pNF-κB-Luc, and/or 100 ng of pFC-MEKK (Stratagene, La Jolla, CA). Cells were treated with either 1 μM ATO (A) or 1 μM APO (B), and an FL assay was performed 24 h later. The results shown are means from three independent experiments. The relative FL activity is shown. (C and D) Effect of ATO or APO on the AP-1 signaling pathway. O cells were transfected with 100 ng of pAP-1-Luc and/or 100 ng of pFC-MEKK (Stratagene). Cells were treated with either 1 μM ATO (C) or 1 μM APO (D), and an FL assay was performed 24 h later as described for panels A and B. (E) Effect of ATO on the phosphorylation level of STAT3 at tyrosine 705. The results of Western blot analysis of cellular lysates with anti-phospho-STAT3 (Tyr705), anti-STAT3, or anti-β-actin antibody in O cells treated with either 1 μM ATO or 1 μM APO for 24 h are shown. (F) Effect of ATO on the STAT3 signaling pathway. O cells were transfected with 100 ng of STAT3 reporter APRE-Luc (41) (STAT3-Luc, a generous gift from T. Hirano, Osaka University, Japan). Cells were treated with 1 μM ATO for 19 h and then stimulated with 100 ng/ml of interleukin-6 for 5 h, and an FL assay was performed as described for panels A and B.

level was suppressed by about 30% compared with that of the control cells, and this occurred without cell toxicity (data not shown). However, consistent with previous reports in which ATO-induced apoptosis was enhanced by BSO (14, 20, 33), most of the cells died, possibly through apoptosis, when the OR6 cells were cotreated with 1 μM ATO and 1 μM BSO for 72 h (data not shown), suggesting that ATO and BSO synergistically generate ROS and deplete glutathione, resulting in induction of oxidative damage. Taken together, these results suggest that ATO may inhibit the HCV RNA replication by modulating the glutathione redox system and oxidative stress.

DISCUSSION

ATO has been reported to affect multiple biological functions, such as PML-NB formation, apoptosis, differentiation, stress response, and viral infection (38). Indeed, ATO has been shown to increase retroviral infectivity, including infectivity of HIV-1, HIV-2, feline immunodeficiency virus, simian immunodeficiency virus from rhesus macaques, and murine leukemia virus, although the mechanisms responsible for these changes are not well understood (5, 6, 32, 44, 47, 50, 57). PML, which is involved in host antiviral defenses, is required for the formation of the PML-NB, which is often disrupted or sequestered in the cytoplasm by infection with DNA or RNA viruses (17). The fact that ATO promotes the degradation of PML and alters the morphology or distribution of PML-NBs suggests that ATO enhances HIV-1 infection by antagonizing an antiviral activity associated with PML. In fact, HIV-1 infection has been reported to alter PML localization (57), although others have failed to confirm this finding (5). Furthermore, Berthoux et al. demonstrated that ATO stimulated retroviral reverse transcription (5). Moreover, ATO has been shown to have an inhibitory effect on host restriction factors, such as TRIM5a, Ref1, and Lv1, in a cell type-dependent manner (5, 6, 32, 44, 47, 50). In contrast, we have demonstrated that ATO strongly inhibited genome-length HCV RNA replication without cell toxicity (Fig. 1A and 2A). In addition, we observed the cytoplasmic translocation of PML in the HCV RNA-replicating O cells after the treatment with ATO (Fig. 4A). However, PML was dispensable for the anti-HCV activity of ATO as well as HCV RNA replication (Fig. 4E). In this regard, it is worth noting the recent report by Herzer et al. that the HCV core protein interacts with PML isoform IV and abrogates the PML function (22). Thus, PML may be involved in the HCV life cycle. In any case, the sensitivity to ATO and the cellular target of ATO seem to be different between HCV and HIV-1.

HCV infection has been shown to cause a state of chronic oxidative stress like that seen in chronic hepatitis C, which may contribute to fibrosis and carcinogenesis in the liver (16, 18, 40). In particular, HCV replication has been associated with the endoplasmic reticulum (ER), where HCV causes ER stress. Indeed, HCV NS5A and core, the ER-associated proteins, have been reported to trigger ER stress (4, 55). Therefore, HCV infection causes production of ROS and lowering of mitochondrial transmembrane potential through calcium signaling (4, 36). Among the HCV proteins, core, E1, NS3, and NS5A have been shown to be potent ROS inducers, and these HCV proteins also alter intracellular calcium levels and induce oxidative stress, thereby inducing DNA damage, and constitu-